


# Centennial-scale lake-level lowstand at Lake Uddelermeer (The Netherlands) indicates changes in moisture source region prior to the 2.8-kyr event

The Holocene  
2016, Vol. 26(7) 1075–1091  
© The Author(s) 2016  
Reprints and permissions:  
sagepub.co.uk/journalsPermissions.nav  
DOI: 10.1177/0959683616632890  
hol.sagepub.com  


S Engels,<sup>1</sup> MAJ Bakker,<sup>2</sup> SJP Bohncke,<sup>3</sup> C Cerli,<sup>1</sup> WZ Hoek,<sup>4</sup>  
B Jansen,<sup>1</sup> T Peters,<sup>1</sup> H Renssen,<sup>3</sup> D Sachse,<sup>5</sup> JM van Aken,<sup>4</sup>  
V van den Bos,<sup>1</sup> B van Geel,<sup>1</sup> R van Oostrom,<sup>1</sup> T Winkels<sup>4</sup>  
and M Wolma<sup>1</sup>

## Abstract

The Uddelermeer is a unique lake for The Netherlands, containing a sediment record that continuously registered environmental and climatic change from the late Pleistocene on to the present. A 15.6-m-long sediment record was retrieved from the deepest part of the sedimentary basin and an age–depth model was developed using radiocarbon dating, <sup>210</sup>Pb dating, and Bayesian modeling. Lake-level change was reconstructed using a novel combination of high-resolution palaeoecological proxies (e.g. pollen, non-pollen palynomorphs, chironomids), quantitative determinations of lake-level change (ground-penetrating radar), and estimates of changes in precipitation (lipid biomarker stable isotopes). We conclude that lake levels were at least as high as present-day water levels from the late glacial to 3150 cal. yr BP, with the exception of at least one lake-level lowstand during the Preboreal period. Lake levels were ca. 2.5 m lower than at present between 3150 and 2800 cal. yr BP, which might have been the result of a change in moisture source region prior to the so-called 2.8-kyr event. Increasing precipitation amounts around 2800 cal. yr BP resulted in a lake-level rise of about 3.5–4 m to levels that were 1–1.5 m higher than at present, in line with increased precipitation levels as inferred for the 2.8-kyr event from nearby raised bog areas as well as with reconstructions of higher lake levels in the French Alps, all of which have been previously attributed to a phase of decreased solar activity. Lake levels decreased to their present level only during recent times, although the exact timing of the drop in lake levels is unclear.

## Keywords

2.8-kyr event, chironomids, deuterium, ground-penetrating radar, lake level, late Holocene, lowstand, *n*-alkanes, The Netherlands

Received 7 July 2015; revised manuscript accepted 4 January 2016

## Introduction

Model studies indicate that human-induced climate change will affect precipitation patterns across the globe (IPCC, 2013), but the processes that drive changes in precipitation patterns on a regional scale are not yet well understood (Zhang et al., 2007). To improve our understanding of these regional changes, a critical analysis of the mechanisms behind past changes in temporal and spatial precipitation patterns is essential. A wide range of proxies and techniques is available to reconstruct such past changes in the climate system, and lake sediments provide natural archives in which these proxies are preserved.

One of the most well-established approaches for precipitation reconstruction is the interpretation of (lacustrine) palaeoecological datasets such as pollen records in the context of hydrological demands of indicator taxa. For example, the rapid decrease in hemlock (*Tsuga*) at 5500 cal. yr BP throughout eastern North America has been interpreted to be the result of increased aridity (Shuman et al., 2004, 2009). Over the last decades, there has been major progress in the development of new proxies for reconstructing past precipitation. First, the analysis of sedimentary disconformities, originally studied through series of sediment cores

(e.g. Digerfeldt, 1986) and more recently by ground-penetrating radar (GPR) imaging (e.g. Newby et al., 2009), can be used to obtain quantitative evidence of past lake-level changes (i.e. meters magnitude). Additionally, a sedimentary approach using

<sup>1</sup>Institute for Biodiversity and Ecosystem Dynamics, University of Amsterdam, The Netherlands

<sup>2</sup>TNO Geological Survey of the Netherlands, The Netherlands

<sup>3</sup>Section Climate Change and Landscape Dynamics, Department of Earth Sciences, VU University Amsterdam, The Netherlands

<sup>4</sup>Department of Physical Geography, Faculty of Geosciences, Utrecht University, The Netherlands

<sup>5</sup>Section 5.1: Geomorphology, Helmholtz Centre Potsdam, GFZ German Research Centre for Geosciences, Germany

## Corresponding author:

S Engels, Institute for Biodiversity and Ecosystem Dynamics, University of Amsterdam, Science Park 904, 1098 XH Amsterdam, The Netherlands.

Email: stefanengels.work@gmail.com

the macroscopic components of lake marl allows the quantitative reconstruction of lake-level fluctuations (Magny, 2013). Second, recently, there has been major progress in quantitative lake-level reconstructions using the transfer function approach (e.g. Birks et al., 2010). For instance, the application of transfer functions to fossil chironomid and cladoceran records obtained from shallow lakes can be used to produce continuous and quantitative estimates of past lake levels, in the absence of large shifts in other factors affecting the invertebrate fauna (Engels et al., 2012; Nevalainen and Luoto, 2012). As a third and final example, recent advances in organic geochemistry now enable us to measure compound-specific hydrogen-isotope ratios (expressed as delta-Deuterium or  $\delta D$  values) of lipids that themselves are biomarkers for certain (groups of) species. An exciting application of such an analysis of compound-specific hydrogen-isotope ratios of lipid biomarkers as a proxy for past precipitation is provided by Rach et al. (2014). Rach et al. (2014) were able to reconstruct the stepwise adaptation of the circulation pattern over NW Europe to the temperature decrease that marked the onset of the Younger Dryas (YD) by comparing the  $\delta D$  values of lipid biomarkers assumed to have derived from terrestrial vegetation (e.g. long-chain alkanes such as  $nC_{29}$  as also measured in this study; see below) with the  $\delta D$  values of lipids derived from aquatic vegetation (short-chain alkanes such as  $nC_{23}$ ; not measured in this study).

Several qualitative reconstructions of changes in effective precipitation (precipitation minus evapotranspiration) based on palynological and macrofossil analysis applied to lacustrine sediment records are available for the Netherlands. Bohncke and Wijmstra (1988) reconstructed rapid changes in lake levels during the late glacial for three individual lakes in The Netherlands, including lake Uddelermeer. Their results show lake-level lowerings during the Older Dryas, late Allerød, and the end of the YD. Bos et al. (2006) used multiple sediment records from a former lake in the south of the Netherlands and showed a dynamic lake-level history during the late glacial, mirroring the results by Bohncke and Wijmstra (1988). The results of both these studies do not cover the Holocene. Bos et al. (2007) used a combination of five lake and peat records from The Netherlands to reconstruct early Holocene changes in effective precipitation. These authors showed the occurrence of a period characterized by dry continental conditions between 11,430 and 11,350 cal. yr BP, the so-called Rammebeek phase, based on the occurrence of an increase in grass pollen in all palynological records. The late Preboreal showed a shift to more humid conditions, as indicated by local *Sphagnum* peat growth, but the records presented by Bos et al. (2007) do not extend beyond the early Holocene. Finally, Bohncke (1991) showed the only reconstruction of Holocene lake-level change using a sediment record obtained from Dutch lake Mekelermeer. He based his reconstruction on the ratio of different aquatic palynomorphs (e.g. pollen of aquatic macrophytes and shoreplants, moss spores, and algal remains). His reconstruction shows 18 phases of lake-level lowstands and 18 phases of highstands, but no estimates of the magnitude of change could be made. Accordingly, so far, no quantitative lake-level reconstructions that cover the Holocene period are available for The Netherlands.

The 2.8-kyr BP climate event (2.8-kyr event), previously often referred to as the ‘Subboreal–Subatlantic climate transition’, is one of the most prominent Holocene climate shifts recognized in NW Europe. Van Geel et al. (1996) and Engels and Van Geel (2012) summarized evidence for climatic change around the 2.8-kyr BP event and show that peat bog profiles from Ireland to The Netherlands, Germany, and further east to Poland and north to Fennoscandia are characterized by a transition from so-called ‘Older *Sphagnum* peat’ to ‘Younger *Sphagnum* peat’ (e.g. Dupont, 1985; Van Geel, 1978) at the 2.8-kyr event. This transition was most likely caused by an increase in precipitation, as taxa that are typical for relatively dry conditions (e.g. *Sphagnum* species of the

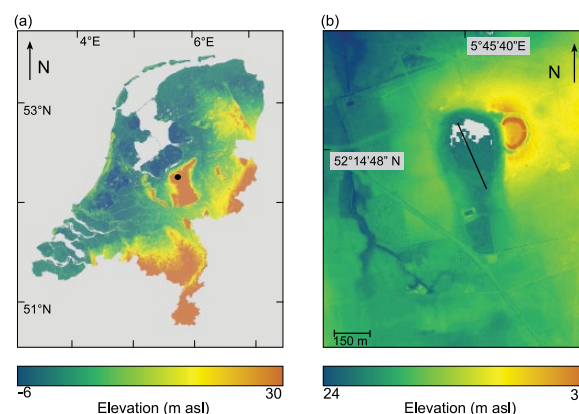


**Figure 1.** (a) Location map of Uddelermeer. Background is the Dutch Digital Elevation Model ahn2 (<http://www.ahn.nl>); (b) local setting of Uddelermeer with the man-made ‘Huneschans’ (defensive structure) on the east bank of the lake. The location of the GPR profile is indicated by the black line.

section *Acutifolia*) are replaced by relatively wet-indicating taxa (e.g. *Sphagnum cuspidatum*, *Sphagnum papillosum*). The 2.8-kyr event has been dated using detailed radiocarbon studies in peat bogs (e.g. Van Geel et al., 1998, 2014) to 2850 cal. yr BP. More evidence for an increase in precipitation in Europe at 2850 cal. yr BP is derived from lake-level studies in the French Alps (e.g. Magny, 2006) and by a recent study of a varved sediment record obtained from lake Meerfelder Maar, Germany (Martín-Puertas et al., 2012). All of the combined evidence suggests increased precipitation levels across the 2.8-kyr BP event, but the magnitude of change is still unclear. Second, outside of the changes observed for the 2.8-kyr BP event, surprisingly little evidence of middle to late Holocene changes in precipitation is available for Europe. This can either be seen as evidence for a very stable Holocene climate in Europe, but in contrast it could reflect the insensitivity of certain of the proxy-indicators that were previously used to reconstruct past precipitation.

In this paper, we report the results of applying a combination of well-established palaeoecological and sedimentological proxies (e.g. pollen, loss-on-ignition (LOI)) as well as novel techniques (including GPR imaging, hydrogen-isotope analysis) to the late glacial and Holocene sediment record of Uddelermeer (The Netherlands). This selection of proxies allows us to combine high-resolution qualitative indicators of lake-level change (e.g. chironomids) with quantitative methods (e.g. GPR). Including the analysis of the hydrogen-isotope ratio of a lipid biomarker that reflects the terrestrial vegetation in this study will also allow us to directly compare our lake-level reconstruction against a record of changes in precipitation. We specifically aim to reconstruct the yet unknown late Holocene lake-level history for the Netherlands.

## Site description

The Uddelermeer is situated in the central part of The Netherlands (N 52°14'48"; E 5°45'40") in a relatively low position between two push moraines of Saalian age (Figure 1a). Because of this situation, the Uddelermeer area is a focal point for groundwater flow. Water levels of groundwater-fed lakes such as the Uddelermeer are sensitive to changes in effective precipitation.

The push moraines as well as the non-glacial sediments (including slope deposits and cover sands) consist mostly of coarse grained gravelly sands. In this hydrogeological setting, two pingos developed when permafrost conditions reigned during the Last Glacial Maximum (LGM). The large ice lenses and permafrost disappeared after the LGM, leaving behind two basins

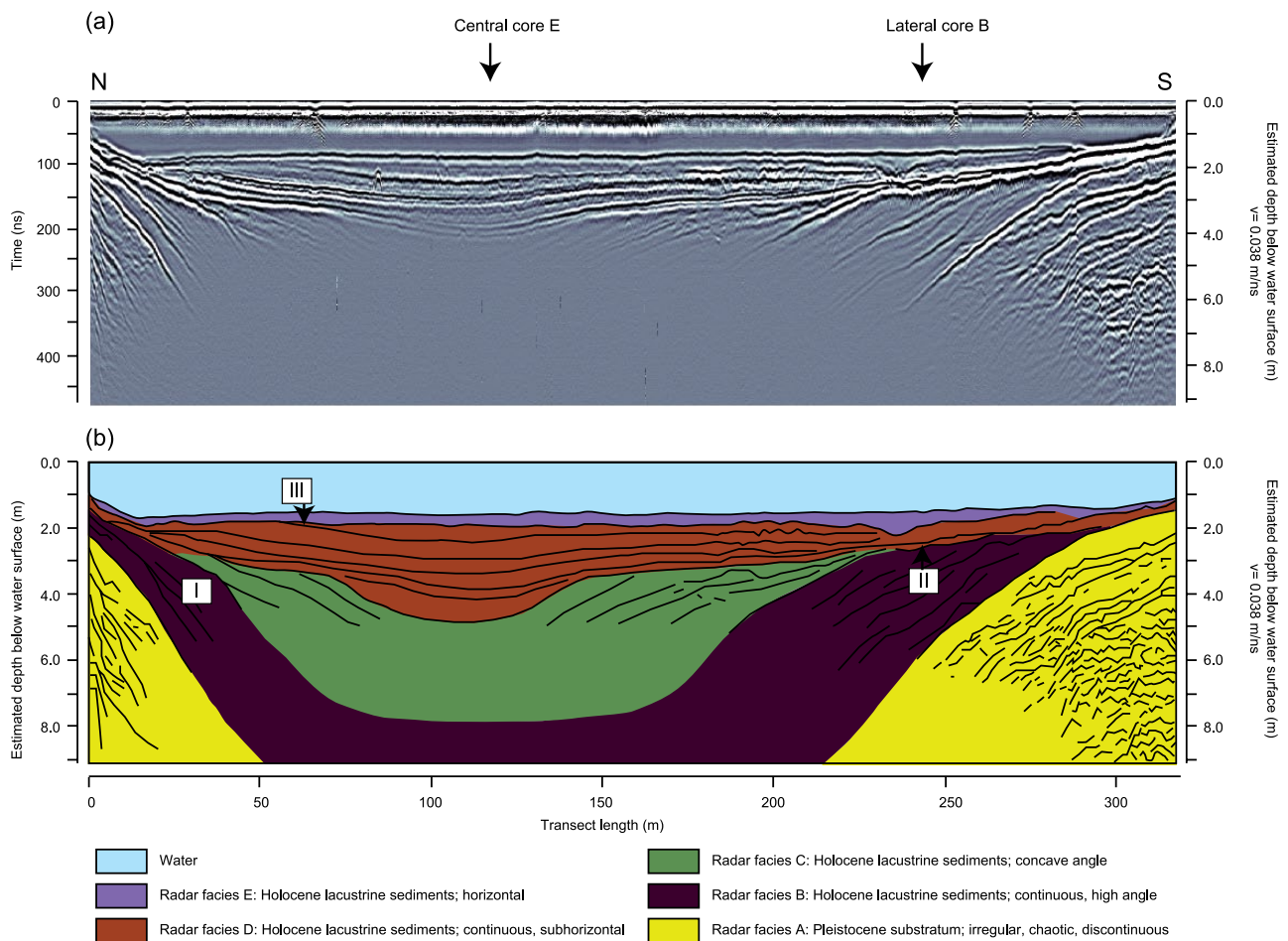


**Figure 2.** (a) Ground-penetrating radar profile (100 MHz) across Uddelermeer (see Figure 1b for location of transect) and the location of the sediment cores used in this study; (b) interpretation of the GPR profile. Roman numerals (I–III) and radar facies (A–E) mark sedimentary discontinuities discussed in the text.

that subsequently altered into lakes: Uddelermeer and Bleeke-meer. Uddelermeer is the largest of the two lakes, with a long axis of ~300 m and a current water depth of 1.3 m. In the surroundings of Uddelermeer, Weichselian cover sands occur at the surface, and the area is nowadays characterized by intense agricultural activity. The lake is bordered by stands of trees (mostly *Alnus*) on the west and a small fringe of wetlands to the north, northeast, and south. A small beach was constructed on the southeast end of the lake, but recreational activity is currently prohibited because of blooms of toxic cyanobacteria in the summer period. A small (canalized) stream drains the Uddelermeer on its southern edge.

A large man-made defensive structure (‘ringfort’) called the Huneschans is situated at the eastern border of the lake. It was most likely constructed to protect iron ore trade. The Huneschans was probably constructed during medieval times (construction is dated to AD 950–1050; Heidinga, 1987). It consists of two circular defensive walls with a moat. The walls and moat do not form a complete circle, but most likely the ‘horseshoe-shaped’ structure bordered the lake during time of construction and use. The moat is currently not carrying water, and the Huneschans is nowadays situated ca. 25 m away from the lake shore (Figure 1b).

## Materials and methods

### GPR imaging and sediment coring

GPR data were acquired using Pulse EKKO Pro equipment in a common offset setup. The survey was carried out on winter ice (February 2012) that enabled easy access. The applied 100-MHz antennae were able to penetrate through the ice, the water column,

and into the sub-bottom sediments to a maximum depth of ~8 m below the surface. Diffractions were used to estimate the sub-bottom signal velocity. Radar facies (reflection patterns) and reflection terminations were of key interest in the unraveling of the sedimentation record. The radar imagery shows a clear contrast between the Pleistocene substrate (with chaotic reflection patterns), several sets of lake infill (continuous reflections sets and terminations), and the overlying water column (transparent facies with occasional diffractions because of cracks in the ice). The insights gained by the use of GPR were used to allocate strategic drilling sites and were also of use in the process of sampling, analysis, and interpretation of the borehole data.

Two overlapping sediment sequences were extruded from the deepest part of the sedimentary basin using a 3-m-long UWITEC piston corer (core sequences UDD-E and UDD-F) from a floating platform during fieldwork in April and May 2012 (central core in Figure 2). Core E reached down to a sediment depth of 1500 cm and failed to reach the top of the Pleistocene sands underlying the lacustrine infill of the lake basin. Core F reached down to 1605 cm sediment depth and did reach into the Pleistocene sands (top of sands = 1540 cm sediment depth). Three additional sediment sequences (core sequences UDD-A to UDD-C; only sequence UDD-B shown in Figure 2) were obtained from core locations situated on a N-S transect across the lake, selected to bracket sedimentary discontinuities visible on the GPR profile (roman numeral ‘II’ in Figure 2a; see below). The 3-m-long core segments were partitioned into 1-m-long segments at the site and stored in a cold room awaiting further analysis. A Glew corer and a Niederreiter gravity corer were used to obtain undisturbed sediment sequences from the uppermost part of the sediment record.

**Table 1.** AMS  $^{14}\text{C}$  ages of dated macroremains from the Uddelermeer basin.

	Core	Sediment depth (cm)	Dated material	Lab ID	$^{14}\text{C}$ age (BP)	Age (cal. yr BP)
1	UDD-E	147–154	Wood frag	GrA-60728	645 ± 50	
2	UDD-E	177–183	<i>Calluna</i> twigs	GrA-60729	1200 ± 130	
3	UDD-E	208–215	<i>Calluna</i> twigs	GrA-60730	1170 ± 40	
4 <sup>a</sup>	UDD-E	291–294	<i>Betula</i> fs (4); <i>Carex</i> fs (1); <i>Calluna</i> twigs; charred wood frag.	GrA-60671	3765 ± 40	
5	UDD-E	416–424	Wood frag; charcoal	GrA-60702	1910 ± 35	
6	UDD-E	486–494	<i>Calluna</i> twigs; charcoal	GrA-60672	2395 ± 40	
7	UDD-E	550–559	<i>Calluna</i> twigs; <i>Calluna</i> florescence; <i>Erica</i> florescence; Asteraceae fs; charred twig	GrA-60673	2410 ± 35	
8 <sup>a</sup>	UDD-E	586–594	<i>Betula</i> fs (2); <i>Betula</i> catkin scale; <i>Calluna</i> twigs; <i>Lycopus</i> fs (3); <i>Mentha</i> fs (1) leaf fragments; wood frag; charred wood frag.	GrA-60674	3965 ± 40	
9	UDD-E	647–654	<i>Betula</i> fs (4); <i>Callitriche</i> fs (2); <i>Calluna</i> twigs; <i>Hydrocotyle</i> fs (2); leaf frag; wood frag; charcoal	GrA-60676	2855 ± 35	
10	UDD-E	687–694	leaf frag; wood frag; charcoal	GrA-60732	3700 ± 50	
11	UDD-E	777–783	<i>Betula</i> fs (6); <i>Calluna</i> twigs; leaf frag; charred grass; charred leaves; charcoal	GrA-60678	3530 ± 35	
12	UDD-E	888–893	<i>Betula</i> fs (2); leaf frag; charcoal	GrA-60734	5080 ± 100	
13	UDD-E	947–953	<i>Betula</i> fs (1); wood frag	GrA-60749	Failed	
14	UDD-E	987–994	<i>Betula</i> fs (1); charcoal	GrA-60751	5790 ± 80	
15	UDD-E	1088–1095	<i>Betula</i> fs (1); <i>Betula</i> catkin scale; <i>Lycopus</i> fs (1); charcoal	NA	Failed	
16	UDD-E	1188–1195	<i>Pinus</i> epidermis; Charcoal	NA	Failed	
17	UDD-E	1247–1254	<i>Betula</i> fs (7); Leaf frag; wood frag; charcoal	GrA-60735	9500 ± 70	
18 <sup>a</sup>	UDD-E	1457–1463	<i>Betula</i> fs (3); <i>Pinus</i> epidermis	GrA-60748	8680 ± 60	
19	UDD-E	1492–1498	<i>Betula</i> fs (11); <i>Betula</i> catkin scale (1); leaf frag	GrA-60736	11890 ± 80	
20	UDD-F	1550–1554	<i>Alnus</i> fs (1); <i>Carex</i> fs (6); wood frag	GrA-60680	Failed	
21	UDD-B	72–76	<i>Calluna</i> twigs; fern leaf; Leaf frag; wood frag; charcoal	GrA-60681	2705 ± 35	2860–2750
22	UDD-B	76–78	Wood frag; <i>Carex</i> fs (1)	GrA-60682	2570 ± 35	2760–2500
23	UDD-B	81–85	Charcoal	GrA-60683	3590 ± 40	4070–3730
24 <sup>a</sup>	UDD-B	87–89	<i>Betula</i> fs (1); <i>Carex</i> fs (1); wood frag; charcoal	GrA-60684	4370 ± 40	5040–4850
25	UDD-B	89–91	Wood frag	GrA-60687	3440 ± 40	3830–3610
26	UDD-gully	24–26	<i>Betula</i> fs; <i>Poa</i> fs; Leaf frag	GrA-62323	35 ± 20	

GrA: Groningen Centre for Isotope Research; frag: fragments; fs: fruits/seeds.

Cores UDD-E and UDD-F make up the central core sequence; UDD-B is the lateral core described in the text; UDD-gully is a sample taken from the organic infill of the outflow on the southern end of lake Uddelermeer. Radiocarbon dates were converted into calendar years using OxCal v4.2 and the IntCal13 calibration curve (2 sigma; Bronk Ramsey, 2009; Reimer et al., 2013). Dates in the right column are rounded to the nearest decade.

<sup>a</sup>Date identified as outlier.

In this paper, we present results obtained from a combined central sediment sequence as well as from a core taken from the littoral zone. We combined the results from central cores F (1578–1440 cm sediment depth), E (1440–67 cm sediment depth), and gravity core E1 (67–0 cm sediment depth) by matching their LOI records to obtain a master record that covers the entire timespan of the lake ('central core' in Figure 2b). The resulting combined central sequence reaches from the top of the Pleistocene sands at the bottom up to the sediment–water interface. With the exception of more minerogenic sediments near the bottom of the sequence, all material from the central core sequence consists of dark-brown algal gyttja without any visible remains of macrophytes or intercalations of terrigenous material. Core sequence B, located near the southern shore of the lake ('littoral core' in Figure 2b), is 519 cm long and consists of dark-brown organic-rich detrital gyttja with some sandy intercalations, and reached into the underlying Pleistocene sands.

### Chronology

To obtain an accurate chronostratigraphical framework for our data, 26 samples from the upper 67 cm of gravity core E1 were freeze-dried and subjected to  $^{210}\text{Pb}$  measurements following the protocol described in Sanchez-Cabeza and Ruiz-Fernández (2012). We fitted a Constant Flux (CF) Model to the observations in order to create an age–depth model for the uppermost 67 cm of our record.

An additional 20 samples distributed over the entire central core E were selected for AMS  $^{14}\text{C}$  dating (Table 1). The selected material contained organic material reflecting atmospheric  $^{14}\text{C}$  concentrations (such as seeds and fruits from terrestrial plants) as well as charred material (e.g. charred grass epidermis) and charcoal. Because of the presence of some calcite-rich layers in the surrounding push moraine sediments, bulk dating was not considered as a suitable approach for Uddelermeer. As the central core from Uddelermeer was extremely poor in identifiable macrofossils, material from relatively large sediment intervals had to be combined in order to reach an amount sufficient for radiocarbon dating. Despite that effort, four samples failed upon combustion in the lab because of their small size.

Five additional samples were retrieved for radiocarbon dating from the lateral core to bracket a hiatus identified by GPR imagery and palynological analyses (see below). Radiocarbon sample 26 (Table 1) was retrieved from the bottom of the organic infill record of the outflow on the southern edge of Uddelermeer. All radiocarbon dating was performed in the Groningen Centre for Isotope Research.

An age–depth model was constructed for the central core using OxCal software (Bronk Ramsey, 2009), combining the radiocarbon dates from core E with the  $^{210}\text{Pb}$  profile (Figure 3). In this study, calibrated ages for Core E are reported in cal. yr BP with reference to the age–depth model presented in Figure 3. Individual ages for the lateral core and the outflow infill are calibrated using OxCal and reported in cal. yr BP with a 2-sigma error estimate (Table 1).



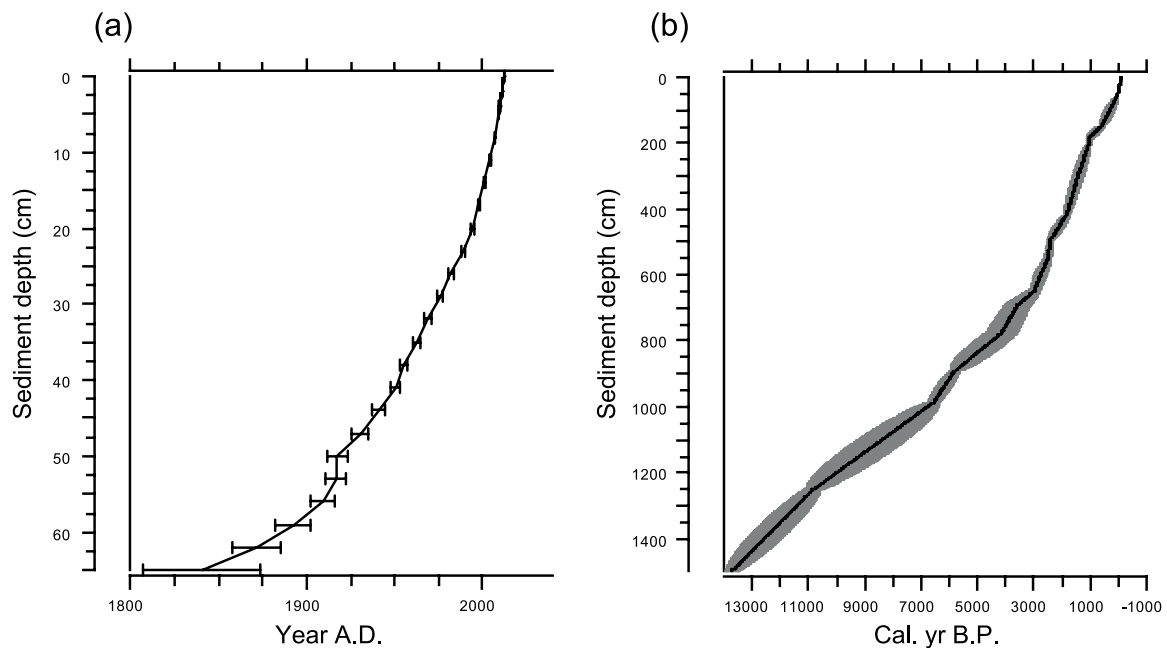


**Figure 3.** (a)  $^{210}\text{Pb}$  profile with fitted CF model; (b) Bayesian age–depth model for central core E, generated using OxCal version 4.2 (Bronk Ramsey, 2009). Radiocarbon dates used in the modeling are presented in Table 1 and were calibrated using the IntCal13 dataset (Reimer et al., 2013).

#### Sedimentological and palaeoecological analysis

LOI was performed on contiguous 1 cm thick samples for the entire E core, totaling to 1412 samples, following the protocol described by Heiri et al. (2001). Wet sediment samples of  $\sim 1.0\text{ cm}^3$  were heated to  $105^\circ\text{C}$  for at least 12 h. After weighing, the dried samples were heated to  $550^\circ\text{C}$  for 4 h to combust all organic matter.

A total of 110 palynological samples were retrieved from the late glacial and Holocene section of central core E. Volumetric samples of  $0.7\text{ cm}^3$  were taken every 10–20 cm and prepared following standard techniques (Faegri and Iversen, 1989; Moore et al., 1991). A *Lycopodium*-tablet was added to each sample in order to enable the calculation of pollen concentration and pollen influx (Stockmarr, 1971). Pollen, fern spores, fungal spores, and other palynomorphs were identified using a light microscope with  $400\times$  magnification ( $1000\times$  when necessary). A reference collection as well as keys and illustrations by Moore et al. (1991) and Beug (2004) was used for pollen identification. The identification of fungal spores and other non-pollen palynomorphs follows Van Geel (1978). A pollen percentage diagram was calculated using a pollen sum ( $n=250$ ) that includes trees and upland herbs and plotted using the TILIA computer program v 1.5.12 (Grimm, 1993, 2004). Pollen zones were identified following the Holocene classification of Mangerud et al. (1974). Fifteen additional samples were selected for palynological analysis from lateral core B and prepared and plotted similar to the core E samples.

In all, 32 samples were selected for chironomid analysis, with a focus on the upper half of the sediment column, as the main aim of this study is the reconstruction of late Holocene lake-level fluctuations. The samples were treated with warm KOH for 15–30 min and subsequently rinsed through a sieve with a  $100\text{-}\mu\text{m}$  mesh. Chironomid head capsules (hcs) and related zoological remains were hand-picked from the residue under  $35\times$  magnification using a Bogorov sorting tray and mounted on permanent slides using Euparal mounting medium. Chironomid head capsules were identified using a light microscope with  $100\times$ – $400\times$  magnification following the taxonomy of Brooks et al. (2007). A chironomid percentage-abundance diagram was constructed using C2 software (Juggins, 2003) and zonation was achieved using optimal sum of squares partitioning as included in the program

ZONE (Lotter and Juggins, 1991), using a broken stick model (as included in BSTICK; Bennett, 1996), to assess the number of significant zones. Square-root-transformed percentage-abundance data were used in a Principal Component Analysis (PCA) in order to explore the data. Rarefaction analysis was performed to assess chironomid taxon richness (TR) for the fossil samples, using the lowest count sum in all counted samples ( $n=73$  hcs). Absolute counting data were doubled prior to analysis to be able to use the rarefaction method that only accepts integers. We used the ‘rarefy’ function as available in the ‘vegan’ package version 2.2 (Oksanen et al., 2015) in R version 3.0.2 (R Development Core Team, 2013) to perform this analysis.

#### Lipid biomarker analysis and hydrogen-isotope ratio ( $\delta\text{D}$ ) determination

A set of 59 samples was taken from the core-interval 956–315 cm depth and freeze-dried prior to lipid biomarker extraction. A Dionex 200 accelerated solvent extraction (ASE) system with 11 mL extraction cells and dichloromethane/methanol (DCM/MeOH) (97:3 v/v) as the extractant was used for extraction of lipid biomarkers. The extract was separated into three fractions: hydrocarbons and esters (solvent: hexane), esters and ketones (solvent: hexane/DCM (4:1 v/v)), and alcohols and fatty acids (solvent: DCM/MeOH (9:1 v/v) following Sachse et al. (2004). A ThermoQuest Trace GC 2000 gas chromatograph connected to a Finnigan Trace MS quadrupole mass spectrometer was used for gas chromatography-mass spectrometry (GC/MS). A volume of  $1.0\text{ }\mu\text{L}$  of the extracts was injected on-column on a 30-m Rtx-5Sil MS column (Restek) with an internal diameter of  $0.25\text{ mm}$  and film thickness of  $0.1\text{ }\mu\text{m}$  to separate the extracts, using He as a carrier gas. Temperature programming consisted of an initial temperature of  $50^\circ\text{C}$  for 2 min, heating at  $40^\circ\text{C}/\text{min}$  to  $80^\circ\text{C}$ , holding at  $80^\circ\text{C}$  for 2 min, heating at  $20^\circ\text{C}/\text{min}$  to  $130^\circ\text{C}$ , immediately followed by heating at  $44^\circ\text{C}/\text{min}$  to  $350^\circ\text{C}$ , and finally holding at  $350^\circ\text{C}$  for 10 min. A mass-to-charge ratio ( $m/z$ ) of 50–650 was used for subsequent MS detection in full scan mode, with a cycle time of 0.65 s and followed electron impact ionization with an ionization energy of  $70\text{ eV}$ . *n*-Alkanes and *n*-alcohols were identified from the chromatograms by their mass spectra and retention times. The peak

areas for each component were compared with the peak areas from the internal standard from the same component class (5 $\alpha$ -androstane for the alkanes and 5 $\alpha$ -androstan-3 $\beta$ -ol for the alcohols) for absolute quantification, assuming a similar response factor within the suite of alkanes and alcohols of different chain length (Jansen et al., 2008).

Compound-specific hydrogen-isotope ratios (expressed as a  $\delta$ D value) of the *n*-alkanes were measured on a Delta-V-Plus Isotope Ratio Mass Spectrometer (IRMS) coupled to a Trace Gas 1310 Chromatograph at the University of Potsdam (Germany). Standardization to the Vienna Standard Mean Ocean Water (VSMOW) scale was carried out using a linear regression function between measured and certified  $\delta$ D values of an *n*-alkane standard mixture (Mix A) obtained from Arndt Schimmelmann (University of Indiana). In addition, we used another certified *n*-alkane mixture (Mix B) to cross-validate standardization results and check for the minimum sample amount needed for reliable measurements. As a result, we only used peaks with a height above 1500 mV for evaluation. The  $H_3^+$  factor as a measure of ion source stability was monitored every day and found to be constant throughout the measurement period. The mean standard deviation of all analyzed A-Mix standards was 2.12‰ ( $n=255$ ) and of all analyzed *n*C<sub>29</sub> alkanes was 0.91‰ ( $n=59$ ). Here, we report the  $\delta$ D-record of the *n*C<sub>29</sub> compound, assumed to reflect terrestrial vegetation as it is commonly encountered in the leaf wax of deciduous plants such as birch or oak.

## Results

### Chronology

Application of CF modeling to the <sup>210</sup>Pb measurements resulted in an age–depth model for the upper 67 cm with relatively small error estimates (<10 years for sediments younger than AD 1900; Figure 3a). However, application of different types of accumulation models (e.g. Constant Sedimentation modeling; Sanchez-Cabeza and Ruiz-Fernández, 2012) results in age estimates that can be offset from the CF model by as much as 20 years near the bottom of the <sup>210</sup>Pb profile.

The age–depth model for the entire central record (Figure 3b) identified at least two of the radiocarbon dates from the E core sequence as outliers (marked in Table 1). The age–depth model for the upper half of the core sequence shows relatively well-constrained age estimates and an almost linear accumulation rate that is relatively high, averaging at ~2.1 mm/yr for the period 2800 cal. yr BP to the present. Because of the very low content of ‘upland’ organic material suitable for radiocarbon dating, the lower half of the sediment sequence only contains five radiocarbon dates. This leads to highly variable age estimates and large associated error estimates. The age–depth model has to be treated cautiously for the depth interval 1540–800 cm (~14–4.5 cal. kyr BP). The chronology of the interval between 4500 cal. yr BP and the present is reliable as long as the error estimates are taken into account ( $\pm 500$ s year for the interval 4500–3000 cal. yr BP;  $\pm 200$ s year between 3000 cal. yr BP and the present).

### Sedimentological analyses

**GPR.** The electromagnetic wave velocity in the sub-bottom sediment record is established at 0.038 m/ns and this low value resembles velocities known in freshwater peats. The depth penetration is 6–9 m. The GPR image shows a clear contrast between the sandy Pleistocene substratum with chaotic, discontinuous reflection patterns (radar facies A; Figure 2) and the lake infill with more continuous and subparallel reflection patterns. The deepest of the radar facies belonging to the lake infill (facies B) consists of low-angle, continuous reflections. Facies C rests unconform on facies B and consists of concave, high-angle reflections. Facies D

rests unconform on facies B and C and consists of subhorizontal reflections. The uppermost facies E is dominated by horizontal reflections sets.

The angular unconformities, expressed by reflector terminations, are interpreted as buried palaeoshorelines and erosional features, probably formed during periods of lake-level lowstand (indicated as I, II, and III in Figure 2) as lake-level lowstands are very likely to have coincided with periods of non-deposition and even erosion. The erosional feature that is visible between 230 and 280 m transect length (roman numeral II, Figure 2) might be related to the buried palaeoshoreline (roman numeral I) as both structures might have formed during the same lake-level lowstand. The sedimentary discontinuity near the top of the profile (roman numeral III, Figure 2) marks the occurrence of a second erosional phase. The sediments that are truncated were most likely deposited during a phase with lake levels higher than at present and were subsequently eroded when lake levels lowered to their current level. The lithology of the sediment cores shows no clear evidence for compaction, clastic sediment influx, growth of vegetation, or other processes that could have led to changes in the sedimentology during these drier regimes.

**LOI.** The LOI profile shows values between 0% and 2% for the glaciofluvial Pleistocene deposits that underlie the lacustrine infill of the pingo remnant (Figure 4; 1600–1540 cm depth). The organic matter content shows increasing values from 5% to peak-values of ~40% in the lowermost part of the sediment sequence (1540–1427 cm depth) before showing an abrupt decrease in variable values of 10–25% between 1427 and 1287 cm depth. LOI values start to increase at 1287 cm depth reaching values of 70% around 1200 cm depth. Organic matter content of the sediments is high and relatively stable up to 860 cm depth, when LOI values start to decrease again. The decrease in LOI continues up to 620 cm depth at which point values of ~50% are reached. From 620 cm depth upward, the LOI increases gradually to values of 80%, before it abruptly declines to values of ~40% at 220 cm depth (coinciding with the transition from facies C to D; Figure 2b). Variable LOI values are observed for the upper 220 cm of the record.

### Palaeoecological analyses

**Pollen – central core.** The onset of the palynological record obtained from the central core shows a reorganization of vegetation that is typical for late glacial pollen diagrams from The Netherlands (Figure 4). The lowermost samples are characterized by high abundances of *Juniperus* and *Betula*, and subsequently *Pinus* reaches high abundances. The pollen assemblages indicate that vegetation around Uddelermeer probably consisted of birch-pine woodlands, a vegetation type typical for the Allerød interstadial in The Netherlands (Hoek, 1997; Van Geel et al., 1989). Although an abrupt decrease in the Arboreal/Non-Arboreal (AP/NAP) ratio is not visible at the onset of the YD in our record, small decreases in percent-abundances of *Betula* and *Pinus*, simultaneous with increases in *Empetrum*, fern spores, and *Artemisia*, indicate the onset of stadial conditions and opening of the birch-pine woodland at 1435 cm sediment depth. An abrupt increase in the AP/NAP ratio at 1280 cm depth marks the onset of the Holocene, and we observe the establishment of birch woodland rapidly followed by birch-pine woodland during the Preboreal (1280–1230 cm depth). A steep increase in *Corylus*-pollen marks the onset of the Boreal (1230–1140 cm depth), followed by the establishment of a deciduous forest consisting of various tree taxa including *Ulmus*, *Quercus*, and *Alnus* during the Atlantic period. The Atlantic period covers 1140–820 cm depth in our record and a decrease in *Ulmus* marks the onset of the Subboreal. First signs of human impact on the vegetation can be seen during the Subboreal (820–525 cm) through the appearance of *Cerealia* and *Plantago lanceolata*.

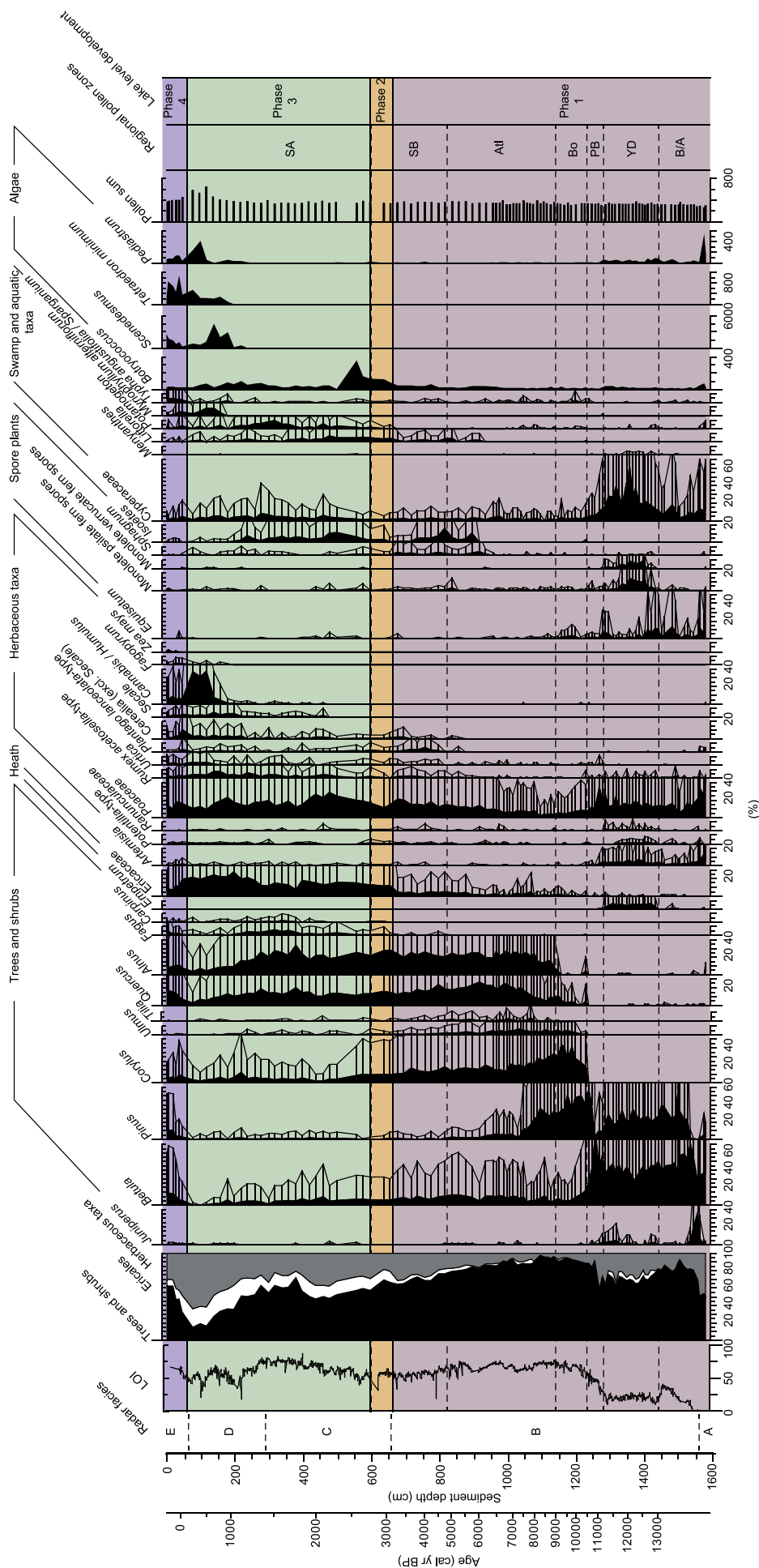


**Figure 4.** Percentage diagram of selected pollen, spore, and algal taxa for central core E of Uddelermeer on a sediment depth scale (cm) with a time scale (cal. yr BP) plotted for reference. Loss-on-ignition profile is plotted to the left of the pollen curves; bio-zonation follows Hoek (1997) for the late glacial and Mangerud et al. (1974) for the Holocene. Phases of lake-level development plotted to the right refer to lake-level high- and lowstands; see text for interpretation.

The decrease in *Corylus* at 525 cm depth is used to identify the Subboreal/Subatlantic transition, and the main diagram subsequently shows a decreasing AP/NAP ratio during the Roman era and a forest recovery during the Migration Period. The uppermost part of our record shows increasing human impact on the vegetation (e.g. decreasing AP-values, increases in Ericaceae and Cerealia) and a strong maximum in *Cannabis/Humulus*-type pollen between 120 and 60 cm depth. Close examination of a number of *Cannabis/Humulus*-type grains using the criteria by Punt and Clarke (1984) indicates that they most likely derived from *Cannabis sativa*, and their sudden appearance in high abundances suggests that the pollen were most likely deposited as the result of retting of hemp in the lake (cf. Slicher van Bath, 1987). A more detailed reconstruction of past vegetation development and local ecosystem response to increasing human impact will be presented elsewhere.

**Pollen – lateral core.** The pollen record of the lateral core (Figure 5) generally resembles the record of the central core. The oldest pollen samples also show an assemblage dominated by *Betula* and *Pinus* and reflect the birch-pine woodland of the Bølling/Allerød interstadial. This is followed by a zone that is characterized by an increase in fern spores, as well as in *Artemisia*, Cyperaceae, and *Empetrum* pollen, taxa that are characteristic of the YD biozone. Unlike in the central core, the YD biozone is immediately followed by a pollen zone in which *Corylus* is the dominant taxon. This implies that the Preboreal period is absent from the lateral core and that the YD sediments are directly overlain by sediments deposited during the Boreal period. Subsequent pollen assemblages indicate that sediments from the Atlantic, Subboreal, and Subatlantic periods can all be recognized in the lateral core, but close inspection and comparison of curves with a characteristic time-development (e.g. *Botryococcus*) show that at least one hiatus of Subboreal age exists in core B (80 cm sediment depth). The presence of a hiatus at 80 cm depth is corroborated by five radiocarbon dates taken just above and just below the hiatus (Table 1) as well as by the GPR data (Figure 2).

**Chironomids.** A total of 52 chironomid taxa were encountered in the 32 chironomid samples taken from the upper half of central core E, and Figure 6 shows all taxa that have a minimum abundance of 2% in at least one sample. The average count sum of the record is 124 hcs per sample (range: 73–288.5). An additional 18 taxa of botanical and zoological macrofossils were encountered and identified in the chironomid samples, and a concentration diagram of these remains is presented in Figure 6b. The almost complete absence of (semi-)terrestrial and stream-indicating chironomids suggests that the lake had no significant inflow and/or that there was no influence of large wetland areas throughout the recorded period. Optimal partitioning zonation indicates the existence of four significant zones in the chironomid record.

Ch-Z1 (800–662 cm sediment depth) is dominated by *Tanytarsus mendax*-type and *Cladotanytarsus mancus* types 1 and 2, with lower abundances of *Lauterborniella*, *Endochironomus albipennis*-type, and *Cricotopus laricomalis*-type. Figure 6b shows a low diversity of other botanical and zoological remains during Ch-Z1. *T. mendax*-type shows an abrupt decline from abundances over 20% to 0–5% at the onset of Ch-Z2 (662–512 cm depth), whereas *Parakiefferiella bathophila*-type and *Pseudochironomus* increase in abundance. Ch-Z2 is also characterized by a more diverse assemblage of other macroremains, including remains of Ephemeroptera, Trichoptera, and Coleoptera. The concentration of chironomid head capsules shows a notable peak at 600 cm sediment depth. The marked increase in *Lauterborniella* together with the decrease in *E. albipennis*-type and *Procladius* at 512 cm sediment depth marks the onset of Ch-Z3. *P. bathophila*-type remains the most abundant taxon during Ch-Z3 (512–262 cm sediment depth),

decreasing in abundance at 262 cm depth, marking the onset of Ch-Z4. *T. mendax*-type and *E. albipennis*-type increase to values similar to those of Ch-Z1 during Ch-Z4 (262–0 cm depth), and *Microtendipes pedellus*-type, *Tanytarsus pallidicornis*-type, *Procladius*, and *Ablabesmyia* all increase in abundance during Ch-Z4.

The zonal transitions are also reflected in the scores of the samples on the first axis of the PCA (Figure 6a). Rarefaction analysis shows high species diversity during phase 1, lower values during phases 2 and 3, and an increase in species richness during the latter half of phase 3, with maximum diversity being reached in the uppermost sample.

**Lipid biomarker  $\delta D$ .** The hydrogen-isotope ratio of *n*-alkane  $nC_{29}$  shows negative values centering at about  $-185\text{‰}$  between 956 and 676 cm depth (Figure 7). From 666 cm depth upward,  $\delta D$  values show a unidirectional shift to less negative values, reaching a new average value of  $-180\text{‰}$  at 596 cm depth. The exact points of change in the record are not easily identified because of the internal variability that is inherently present in the  $\delta D$ -record.

## Discussion

### Reconstruction of late glacial and Holocene lake-level change at Uddelermeer

**Phase I: Late glacial to early Late Holocene (1560–660 cm depth;  $\sim 14,000$ – $3150$  cal. yr BP).** Almost no identifiable terrestrial macroremains suitable for radiocarbon dating could be retrieved from the sediment core between 1560 and 660 cm depth. The chronology for the lower part of the record is therefore based on five radiocarbon dates only and should be treated with caution. The classical late glacial (Hoek, 2001; Van Geel et al., 1981, 1989) and Holocene pollen zones are recognizable in the pollen record of the central core (Figure 4) and provide a means to date the record through biostratigraphical correlation. Because of the lack of a rigorous age–depth model, we discuss the evolution of lake levels during Phase I in terms of biozones (instead of calibrated years BP).

The earliest part of the record shows a relative increase in AP as well as an increase in LOI and the establishment of birch-pine woodland. This development is interrupted at 1425 cm depth when LOI and AP percentages decrease and where *Empetrum*, Cyperaceae, and fern spores increase in abundance. These changes mark the onset of the YD and are visible in both the central core and in the lateral core, suggesting that lake levels were at least as high as today in order to allow for sedimentation of lacustrine sediments even in the (present-day) shallow parts of the lake. The central core shows a subsequent phase of increasing LOI, combined with an increase in *Betula* followed by an increase in *Pinus*. These pollen assemblages, typical for the Preboreal biozone, can be recognized in the central core but are absent in the lateral core (Figure 5). This suggests that either there was no material deposited at the lateral site during the Preboreal or that Preboreal-aged sediments were eroded after deposition. A lowering in lake levels would explain the absence of Preboreal sediments at the lateral coring site, but, because of lack of evidence from other proxy-indicators (e.g. chironomids, GPR), it is unclear by how much lake level had lowered during the Preboreal.

An increase in *Corylus* and subsequent increases in pollen of tree taxa such as *Ulmus*, *Quercus*, and *Alnus* indicate the onset of the Boreal and the Atlantic biozones, respectively. The onset of the Subboreal is less clearly identifiable in our record and is placed at the depth where *Ulmus* decreases in abundance. The chironomid fauna of the early Subboreal is dominated by *T. mendax*-type, a taxon that includes a relatively high number of species and that has therefore been observed in a wide range of environments (Brooks et al., 2007). Clear-water conditions at Uddelermeer are



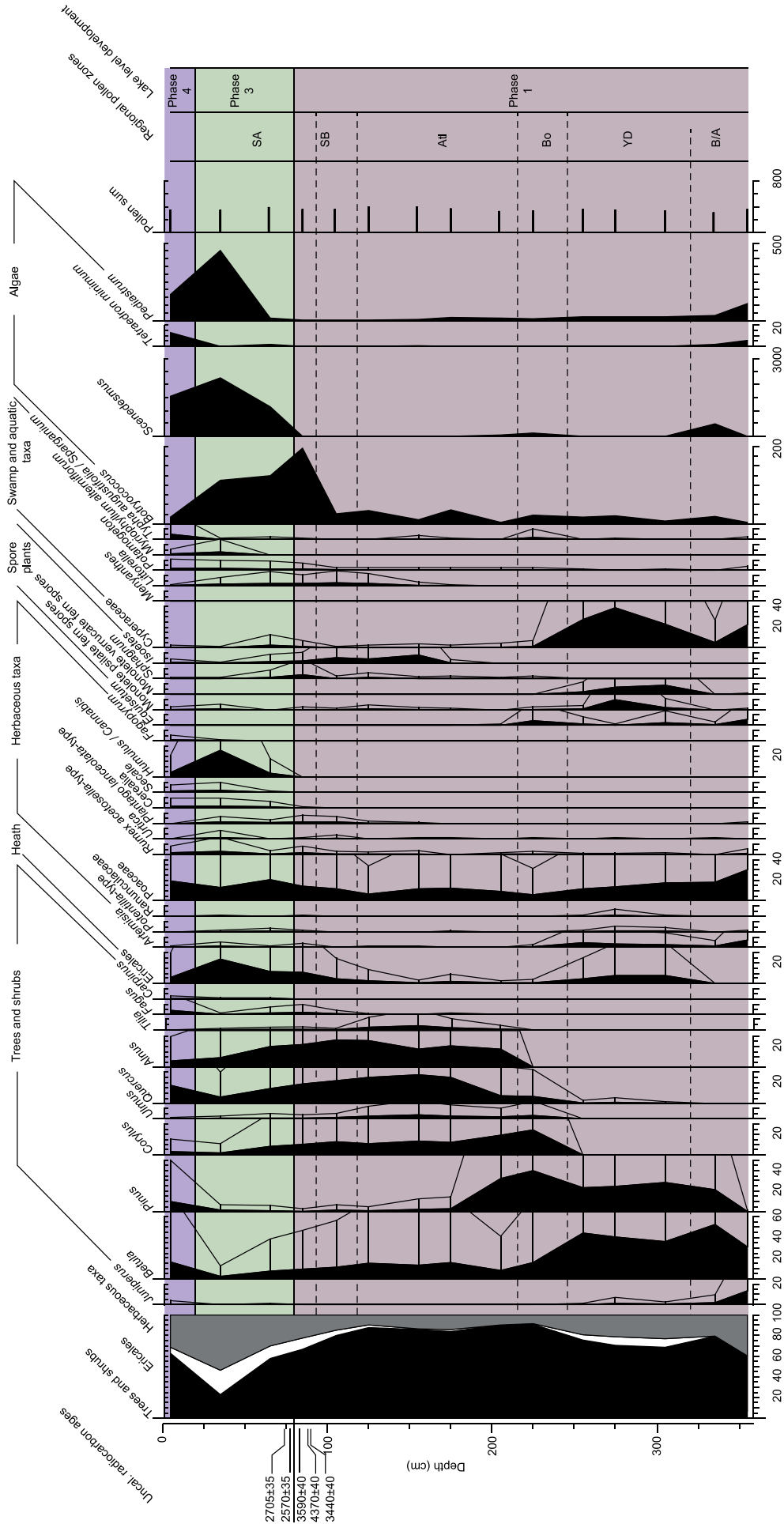


Figure 5. Percentage diagram of selected pollen, spore, and algal taxa for lateral core B of Uddelermeer on a depth scale (cm) with uncalibrated radiocarbon dates plotted to the left (see Table 1). Zonation of the diagram follows Figure 4.

indicated by the presence of *Littorella* and *Isoetes* from the late Atlantic onward. *T. mendax*-type mostly occurs in the profundal zone of shallow oligo- to mesotrophic lakes in the NE American dataset studied by Engels and Cwynar (2011), where it shows highest abundances at water depths deeper than 5 m. *C. mancus*-type also occurs in high abundances during Phase I (Figure 6) and has a preference for littoral habitats (Brooks et al., 2007). The presence of sediments from the Boreal, Atlantic, and Subboreal in both the central and the lateral core, combined with the chironomid fauna that is dominated by a mixture of shallow- and deep-water taxa, suggests that lake levels were at least as high as at present from the Boreal up to the late Subboreal.

**Phase II: Centennial-scale late Subboreal lake-level lowstand (660–600 cm depth; 3150–2800 cal. yr BP).** The chronology of the interval between 4500 cal. yr BP and the present is reliable as long as the (relatively large) error estimates are taken into account, and we therefore discuss the lake-level development from the late Subboreal onward in terms of changes in calibrated years BP.

The GPR profile shows distinct evidence for a lake-level lowstand at the top of radar facies B: reflector terminations indicate the presence of a buried palaeoshoreline at 50 m transect length and ~150 cm sediment depth (roman numeral I, Figure 2). This suggests lowering of the lake level to levels maximum 2.5–3 m lower than the present level. Compaction of the soft lacustrine sediment likely has changed the original elevation of the palaeoshoreline to some extent. A matching palaeoshoreline on the southern end of the transect is not clearly visible in the GPR profile, but sedimentary unconformities between 230 and 280 m transect length indicate the presence of a hiatus that could be related to the lowstand indicated by the buried shoreline on the northern part (roman numeral II, Figure 2). Radiocarbon dates obtained for the lateral core indicate an age of 4070–3610 cal. yr BP for the sediments just below the hiatus in the lateral core (three radiocarbon dates, of which one outlier; Table 1), but oxidation during the lake-level lowstand combined with the erosive effects of wind and precipitation might have resulted in erosion of the exposed (top) sediments. The sediments located just above the hiatus show an age of 2860–2500 cal. yr BP (two radiocarbon dates). Extrapolation of the sedimentary unit associated with the palaeoshoreline visible in the GPR image places the interval of the lowstand at roughly 600–700 cm sediment depth at the location of the central core, suggesting the existence of a water body with a maximum water depth of ~4–5 m during the time of lake-level lowstand. Again, compaction of the soft lacustrine sediment might mean that this estimate is slightly too high.

The GPR image does not have the resolution to allow for a better depth estimate for the onset of Phase II at the location of the central core than 600–700 cm sediment depth. We, however, observe a strong shift in the chironomid assemblages at 660 cm sediment depth with the disappearance of *T. mendax*-type and the appearance of *P. bathophila*-type (Figure 6). This change is accompanied by the appearance of Characeae oospores and a strong increase in abundance of Ericales pollen (Figure 4). We therefore used the depth of 660 cm (3150 cal. yr BP) to define the onset of Phase II (and the transition from radar facies B to C; Figure 2b).

The pollen diagram of central core E shows a clear increase in *Botryococcus* between 660 and 550 cm sediment depth. The chironomid diagram shows increasing headcapsule concentrations and a fauna with a unique combination of high abundances of *Lauterborniella*, *E. albipennis*-type, and *C. mancus*-type between 660 and 600 cm sediment depth (3150–2800 cal. yr BP). All these chironomid taxa are associated with littoral habitats in meso- to eutrophic lakes (Brooks et al., 2007). A lowering of the lake level could have been the main driver of an increase in the ratio of littoral:profundal area and could have resulted in a concentration

of available nutrients because of water volume loss, subsequently leading to eutrophication and increase in blooming of algae such as *Botryococcus*. Oxidation and erosion of exposed lacustrine sediments after lake-level lowering could have provided additional nutrient-input into the lake. The chironomid taxon *T. mendax*-type, indicative of deeper water and less nutrient-rich conditions, disappears from the assemblage at this time too, and additionally, most of the other zoological macroremains (Figure 6b) decrease or disappear from the record during this interval. Decreasing groundwater levels in the area around Uddelermeer could have led to an opening of the vegetation, providing suitable habitats for heath as well as an increase in the availability of clastic material for wind-transport. This would explain the increase in abundance of Ericaceae pollen during Phase II as well as the distinct minimum that can be observed in the LOI record at this time. Finally, the  $\delta D$ -record derived from the  $nC_{29}$  homologue, an  $n$ -alkane formed by terrestrial plants, shows the onset of a new steady state of less negative values during Phase II. Although the magnitude of change at ca. 5‰ is low compared with the magnitude of change observed at the YD/Holocene transition at lake Meerfelder Maar (ca. 20‰; Rach et al., 2014), it is still well outside of the analytical errors of an average 1‰ for the  $nC_{29}$  compound.

Vegetation changes have been suggested to affect  $\delta D$ -records of terrestrial biomarkers (Sachse et al., 2012), in particular changes from C3 to C4 vegetation, which is not, nor was it ever, present at Uddelermeer. Also, data from modern plant samples suggest that C3 grass-derived  $n$ -alkanes are usually characterized by more negative  $\delta D$  values compared with C3 trees growing at the same site (Sachse et al., 2012). However, grasses also produce significantly smaller amounts of  $n$ -alkanes (e.g. Garcin et al., 2014), so this effect may only become apparent in sedimentary archives characterized by an exclusively grass covered catchment. At Uddelermeer, we indeed observe some changes in vegetation during the Subboreal/Subatlantic transition, including a slight decrease in Poaceae after the transition, when  $\delta D$  values already had changed. The changes in the pollen record were, however, much more gradual than the  $\delta D$  shift, and both changes do not coincide in their timing.

A shift toward less negative  $\delta D$  values of the  $nC_{29}$  alkane could therefore be due to either a deuterium enrichment (i.e. less negative values) of the annual precipitation or an increase in plant evapotranspiration as the result of drier conditions (Sachse et al., 2012). As the  $\delta D$ -record shows a shift toward less negative values both during the phase of lower lake levels (phase II) and during the phase of higher lake levels (phase III; see below), we assume that a change in precipitation- $\delta D$  rather than a change in evapotranspiration was the driver of the changes in our  $\delta D$ -record.

Several factors can influence the deuterium enrichment of precipitation. Temperature is an important factor controlling  $\delta D$  of precipitation in temperate regions (Rach et al., 2014; Sachse et al., 2004, 2012). We have not determined the effects of temperature on the  $\delta D$  of precipitation around lake Uddelermeer, but two sites near lake Meerfelder Maar showed a sensitivity of 1.3–2.1‰ in the  $\delta D$  of precipitation per 1°C temperature change (Rach et al., 2014). This would mean that a shift in temperature of 2.4–3.8°C should have occurred in order to explain a 5‰ shift in  $\delta D$  values such as observed for our site. It seems unlikely that a temperature shift of such magnitude occurred given other proxy-evidence that is available from lake Uddelermeer or elsewhere in northwest Europe. We therefore argue that it is more likely that the trend toward less negative  $\delta D$  values was because of a change in the moisture source region and the average moisture pathway length, as transportation distance is an important factor controlling  $\delta D$  values of precipitation (Alley and Cuffey, 2001). Increased transportation distances result in more negative  $\delta D$  values because

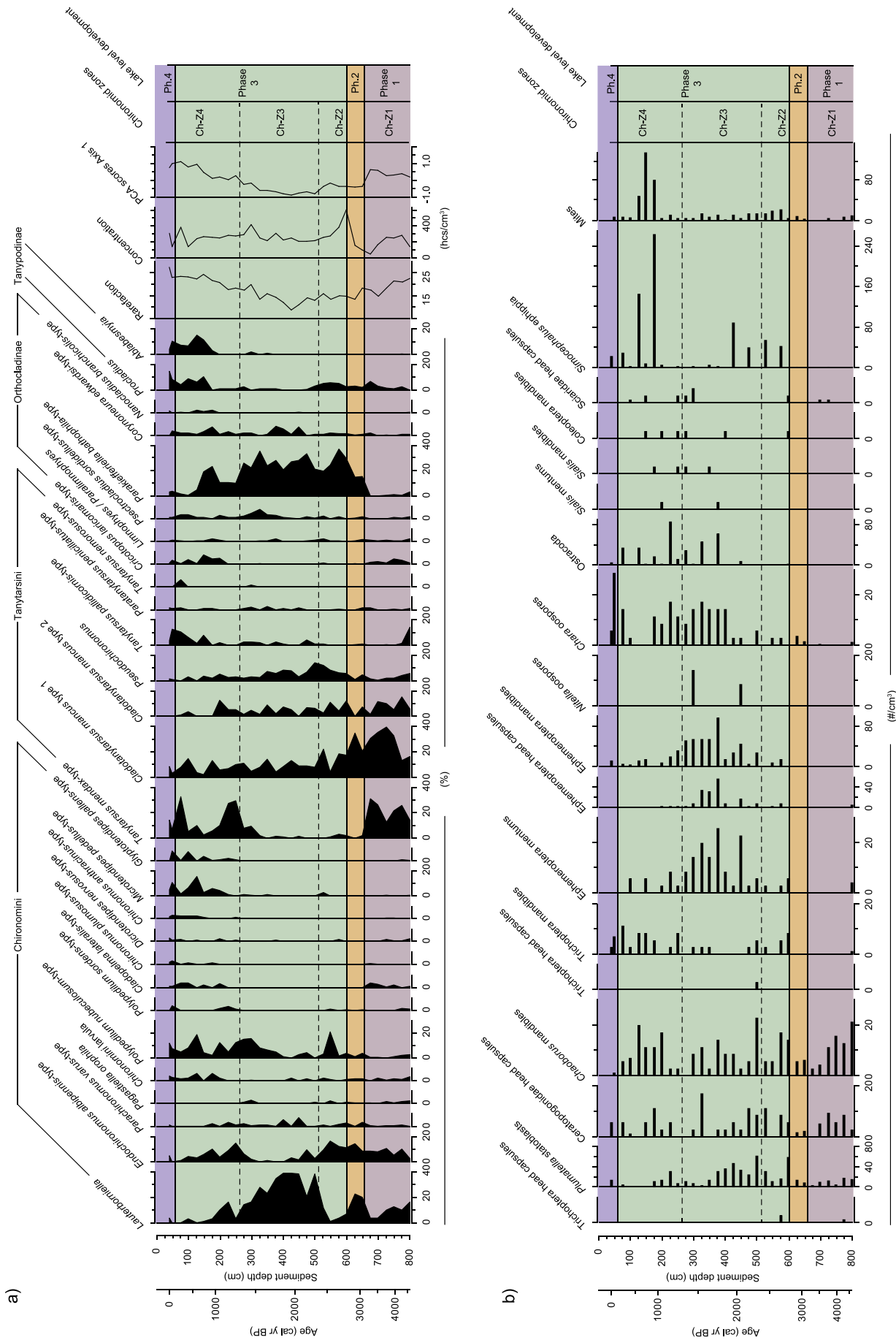


**Figure 6.** (a) Percent-abundance diagram showing chironomid taxa for central core E with at least one occurrence >2%, rarefaction results chironomid concentration, and scores of the chironomid samples on the first axis of a PCA performed with square-root-transformed percentage data; (b) other zoological and botanical macrofossils encountered during chironomid analysis (number/cm<sup>2</sup>). Note the different scalings used for the x-axes. Data are plotted on a depth scale (cm) with a time scale (cal. yr BP) plotted for reference. Zonation was achieved using optimal partitioning; phases plotted to the right follow Figure 4.

of an increased rain-out effect of heavier isotopes, and for our record, a decrease in average transportation distance because of a moisture source region shifting closer to our site could have resulted in the observed shift toward less negative  $\delta D$  values.

Finally, the less negative  $\delta D$  values could also have been the result of a shift in seasonality of rainfall toward more rainfall in the summer period (cf. Sachse et al., 2012). However, as terrestrial plants derive most of their water from rainwater (Rach et al., 2014), and as we assume that the season of lipid-production in the terrestrial vegetation did not change, a change in seasonality of precipitation is unlikely to explain the change to less negative  $\delta D$  values as seen in our record. Concluding, we suggest that the change in  $\delta D$  values toward less negative values was most likely driven by a decrease in the distance to the moisture source, implying changes in the atmospheric circulation pattern from 3150 cal. yr BP onward.

The radiocarbon dates obtained from the lateral core indicate that the phase of lake-level lowstand could have only lasted for a few centuries, as sedimentation at the lateral site started between 2860 and 2500 cal. yr BP.

**Phase III: Subatlantic lake-level highstand (600–58 cm depth; 2800 to ~60 cal. BP).** Lake levels during Phase III were at least as high as today in order to allow sedimentation of organic-rich algal material at the lateral site. Radar facies C and D both were deposited during Phase III, and sedimentary subunits in the lower part of radar facies C suggest that the deepest subbasin (ca. 70–100 m transect length; Figure 2) was preferentially filled in during the earlier part of Phase III (Phase IIIa; Figure 8). Sedimentary unconformities encountered in the upper part of radar facies D indicate that lake levels were even higher than at present (roman numeral III, Figure 2). These subunits are truncated near the current sediment–water interface as a result of subsequent erosion, but extrapolation suggests that water levels might have been 1–1.5 m higher than at present, at least during the later part of Phase III (Phase IIIb). This higher lake level would also match historical maps encountered in old literature (Van Eeden, 1886), would follow contour lines visible in the Dutch Digital Elevation Model (Figure 8 – right hand panels), and would mean that in Medieval times the former lake would have bordered the defensive structure Huneschans, situated on the eastern side of the lake (Figure 8).

The pollen diagram shows little variation in the aquatic micro- and macroflora during phase III. Except for the decrease of *Botryococcus* after the maximum values attained during Phase II, the aquatic vegetation seems surprisingly stable and unresponsive to the relatively large changes in water depth that occurred over the Phase II–Phase III transition. Major changes in the algal community and in the aquatic macrophytes can be observed toward the end of Phase III, which we attribute to increasing human influence on the landscape around Uddelermeer as well as direct influence on the nutrient levels of the lake water through activities such as the retting of hemp (*Cannabis/Humulus* increases to values >30%).

The phase-wise sedimentation history with an initial phase (IIIa) of preferential infilling of a deeper subbasin with the coeval existence of erosional plains at a water depth of ca. 3–4 m (such as between, for example, 220 and 270 m transect length) could potentially be recognized in the chironomid diagram of core E. Chironomid zone Ch-Z2 (662–512 cm) shows an almost complete disappearance of *Lauterborniella*, a shallow-water taxon associated with submerged vegetation (Brooks et al., 2007). It is possible that the erosional plains were initially located at water depths that were too deep to support the aquatic macrophytes that provide suitable habitats for *Lauterborniella* and that these plants could only establish after sedimentation had re-started in the lateral part of the lake basin (Phase IIIb). However, such changes in

aquatic macrophytes cannot be recognized in the pollen diagram of the central core. Chironomid zone Ch-Z3 shows assemblages that are composed of shallow-water taxa such as *P. bathophilatype*, *Lauterborniella*, and *Pseudochironomus*. From 300 cm upward, the increased human influence on the lake ecosystem most likely led to a reorganization of the chironomid fauna, and a direct influence of lake-level fluctuations on the chironomid fauna is no longer recognizable.

**Phase IV: Present-day lake-level lowstand (58–0 cm depth; 60 cal. yr BP–present).** It is obvious from the size of the present-day lake, and the location of the Huneschans with its incomplete circular structure, that the lake level must have dropped between the date of construction of the Huneschans (estimated between AD 850 and 950; Heidinga, 1987) and the present. This lake-level lowering must at least have been in the order of 1–1.3 m based on the difference in height between the moat and the present-day lake level.

Because of the overriding influence of human impact (through increased nutrient loading) on the lake ecosystem, our proxy records have not registered a clear response to the recent lake-level lowering, and it is therefore hard to identify the exact timing of this lowering. Based on the GPR profile, it could be argued that the innermost reflection termination (roman numeral III, Figure 2) marks the transition to radar facies E, which has a base at 60 cm sediment depth at the location of the central core. This depth also coincides with an increase in AP and a decrease in *Cannabis/Humulus* in the pollen diagram, as well as an increase in the LOI record. There are no major changes visible in the chironomid record, but sampling resolution is low in this part. The depth of 60 cm would translate to an age of 60 cal. yr BP (AD 1890; this part of the record is dated using  $^{210}\text{Pb}$  dating), but again the identification of the exact depth and timing of lake-level lowering is difficult because of the overriding effects of factors other than lake depth.

#### Drivers of late glacial and Holocene lake-level fluctuations at Uddelermeer

**Phase I: Late glacial to early late Holocene (1560–660 cm depth; ~14,000–3150 cal. yr BP).** Although we have only limited proxy-information for the earlier part of our record (~14,000–3150 cal. yr BP), we still observe some interesting variations in lake levels of Uddelermeer. The first feature that stands out is that lake levels were high during the YD, as sedimentation of organic-rich algal gyttja occurred even at our lateral coring site. The climate conditions of (the second part of) this biozone are often described as cold and dry (e.g. Dahl and Nesje, 1992; Hoek and Bohncke 2002; Lotter et al., 1992; Rach et al., 2014; Wohlfarth et al., 1994). Detailed studies of lake-level fluctuation on three Dutch sites (including Uddelermeer) revealed an initial increase in lake levels at the onset of the YD, followed by a subsequent and significant lowering of lake levels (Bohncke and Wijmstra, 1988). This pattern of lake-level fluctuations is similar to the one observed for the Swiss Alps by Magny and Bégeot (2004). Despite this evidence for a dynamic precipitation pattern across the YD, we do not observe lake-level fluctuations at Uddelermeer, at least not to the extent that our lateral site was exposed to air. This might be because of the fact that the resolution of our data does not allow the recognition of such changes or that the amplitude of change was not large enough to significantly change lake levels at Uddelermeer.

Lake Uddelermeer shows lake-level lowering during the Preboreal, when our lateral core shows a hiatus. Other Dutch lake records also show evidence of lake-level lowering during the Preboreal (e.g. Bohncke and Wijmstra, 1988; Bos et al., 2007). For instance, the pollen record of lake Hijkermeer (Heiri et al., 2007), located 85 km northeast of Uddelermeer, shows a hiatus

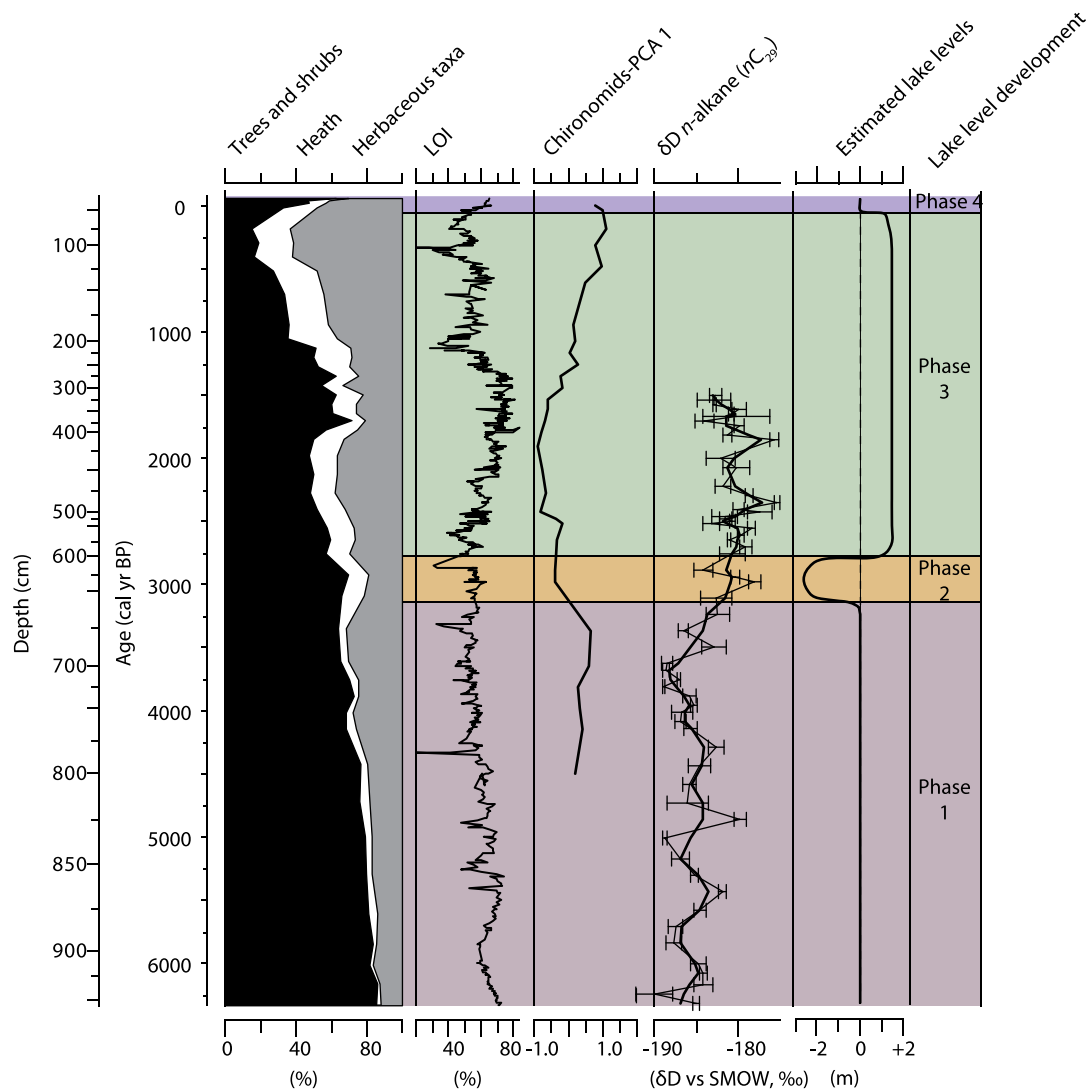


**Figure 7.** Summary figure of proxy records from Uddelermeer (6300 cal. yr BP–present). From left to right: main pollen diagram (%), loss-on-ignition (LOI; %), scores of chironomids samples on first PCA axis, and deuterium:hydrogen ratio ( $\delta D$ ) of lipid biomarker  $nC_{29}$ . Zonation of the diagram follows Figure 4.

with pollen spectra typical for the YD being almost immediately overlain by sediments with increasing abundances of pollen derived from trees taxa that are characteristic of the Atlantic biozone. The climate oscillations that occurred in The Netherlands during the early Holocene included a drier period (Bos et al., 2007; Hoek and Bohncke, 2002), which could have led to a temporary lowering of groundwater levels in The Netherlands, causing lake-level lowering at Uddelermeer.

**Phase II: Centennial-scale late Holocene lake-level lowstand (660–600 cm depth; 3150–2800 cal. yr BP).** The combined evidence from GPR, the palynological analysis, the dating of a hiatus in the lateral core, and the response of the chironomid fauna suggests the occurrence of a lake-level lowstand between 3150 and 2800 cal. yr BP. The first scenario that could explain a lake-level lowering is a period of decreased precipitation, leading to lowering of regional groundwater levels and a reduced lake level at Uddelermeer. Magny (1993, 2004, 2006) provided evidence for regional lowering of lake level in the French pre-Alps and Swiss Plateau region during the late Bronze Age (in his records dated to 3100–2750 cal. yr BP), a result that is similar to our reconstruction of lake-level lowering.

One of the novel aspects of this study is that we were able to determine the  $\delta D$  levels of a lipid biomarker that likely is derived from terrestrial vegetation surrounding the lake. Our  $\delta D$ -record (Figure 7) shows a unidirectional change toward less negative

values, which we interpret to represent a shift in moisture source region, decreasing the average transportation distance of precipitation to our site. We argue that the decreases in lake levels at Uddelermeer might indicate that there was a change in moisture source region and atmospheric circulation pattern across a large part of Europe, just prior to the 2.8-kyr event. These changes in moisture source region might have also affected precipitation levels, possibly having resulted in a decrease in precipitation at Uddelermeer.

A dramatic drainage of the lake might provide another explanation for the lowstand observed at Uddelermeer. Peat bog records retrieved from sites close to Uddelermeer show relatively dry conditions toward the end of the Subboreal period (Van Geel et al., 1996), but no centennial-scale event of extremely dry conditions has been recognized, despite the high-resolution work that has been carried out at, for example, Engbertsdijksvenen (Kilian et al., 1995). A bog burst took place at another nearby raised bog (Bargerveen; Van Geel et al., 2014) across the Subboreal/Subatlantic transition because of oversaturation of the peat bog as a result of excessive rainfall and provides evidence for a non-linear response of ecosystems to climate forcing during the late Holocene. Similar to the situation at Bargerveen, Uddelermeer might have been the subject of an erosional outflow event on the southern end of the lake ('lake burst'). Increasing precipitation amounts could have prompted a partial drainage of the lake and only after



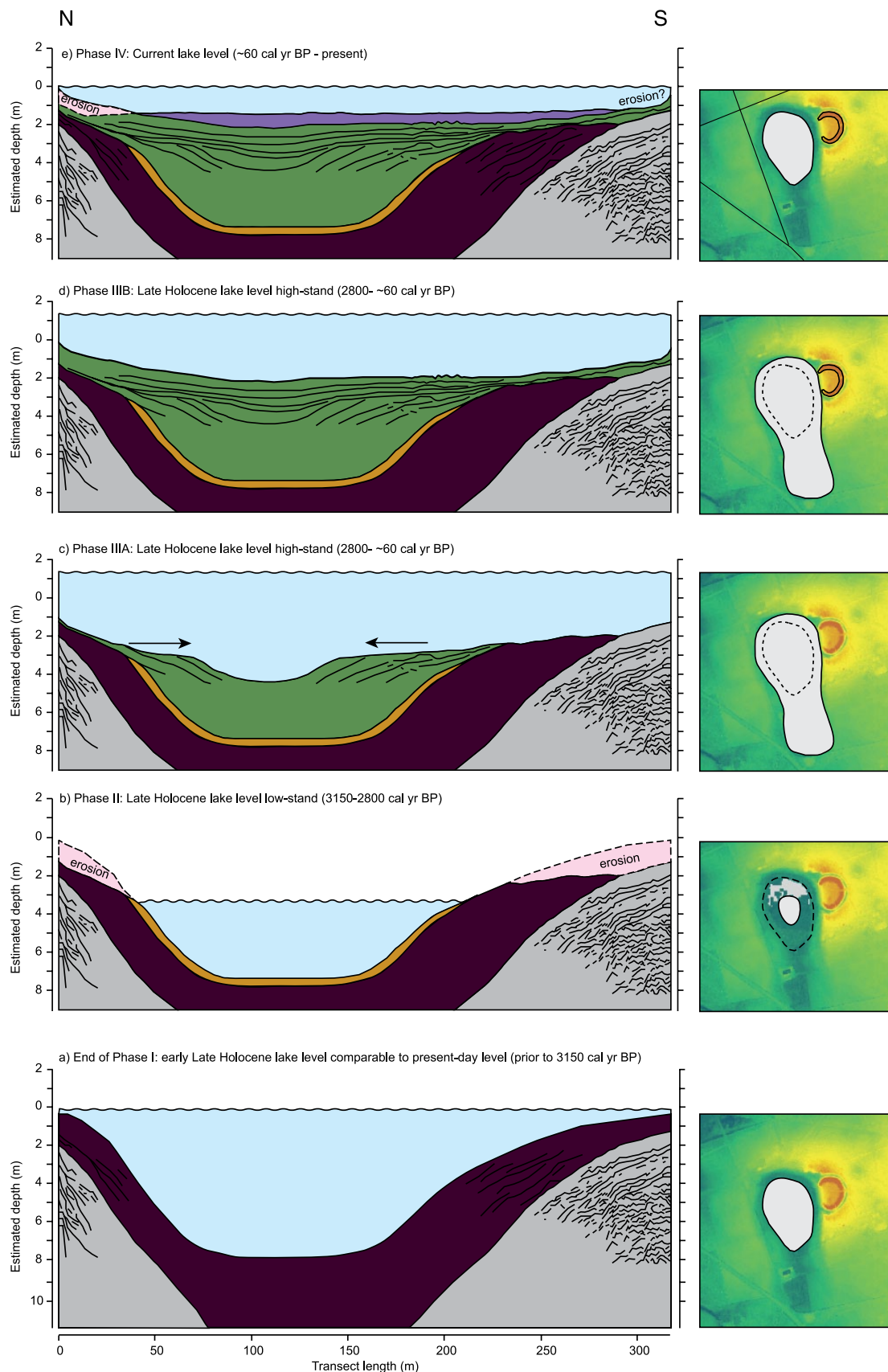


**Figure 8.** Cartoon showing successive phases of lake-level development of Uddelermeer: (a) End of Phase I: Lake level during the early late Holocene (prior to 3150 cal. yr BP) close to present-day levels; (b) Phase II: Centennial-scale late Holocene lake-level lowstand (3150–2800 cal. yr BP) with lake levels ~2.5 m lower than at present and with erosion of exposed areas on the north and south end of the lake; (c) and (d) subsequent late Holocene lake-level highstand (2800 to ~60 cal. yr BP) with lake levels ca. ~1–1.5 m higher than at present; infilling of lake initially concentrated in central subbasin (Phase IIIa) and later vertical sediment accretion across the entire lake (Phase IIIb). Lake borders the archeological defense structure Huneschans after its construction in late Medieval time; (e) Phase IV: Present-day lake levels; erosion in northern end of basin. Lake no longer borders Huneschans. Right-hand side panels show the current elevation map of the area and include the Huneschans to the east of the lake.

subsequent infilling of the outburst channel could lake levels increase to the high lake levels as reconstructed for Phase III. Currently, there is a small (25 cm deep) outflow on the southern end of the lake, but no evidence for the occurrence of an erosional channel has been found so far.

The decrease in lake levels at 3150 cal. yr BP coincides with an increase in Ericaceae pollen, often interpreted to represent increased human impact on the natural vegetation. It is possible that Bronze Age farmers tried to influence the local hydrology by (partially) draining the lake. However, there has been no archeological evidence that supports this hypothesis and the magnitude of lake-level lowering (in the order of several meters) seems rather large.

In conclusion, our data combined with the similar results obtained by Magny (1993, 2004) suggest that there could have been a shift in circulation patterns that affected a large part of Europe already starting prior to the 2.8-kyr event. However, information from other nearby sites is needed in order to establish whether it is an expression of a change in atmospheric circulation patterns affecting a large part of Europe or whether the observed lake-level lowering at Uddelermeer is a strictly local phenomenon.

**Phase III: Subatlantic lake-level highstand (600–58 cm depth; 2800 to ~60 cal. BP).** The increase in lake levels at Uddelermeer coincides, within dating uncertainties, with the 2.8-kyr event at the Subboreal/Subatlantic transition. This transition is characterized by an increase in precipitation in northwest Europe, mainly observed in peat records where a transition from ‘older *Sphagnum* peat’ to ‘younger *Sphagnum* peat’ can be observed (Van Geel, 1978; Van Geel et al., 1996). The ‘older *Sphagnum* peat’ consists of remains of raised bog plants of relatively dry conditions such as *Sphagnum* sect. *Acutifolia*. These relatively dry-indicating taxa are replaced by plants and mosses with increasing moisture demands across the Subboreal/Subatlantic transition, with an initial increase in *S. cuspidatum* and *S. papillosum* followed by an establishment of a vegetation dominated by *Sphagnum imbricatum* (Van Geel, 1978; Van Geel et al., 1996). Pollen records show a distinct decline of *Corylus* over the same interval, which is interpreted as additional evidence for a shift toward wetter conditions.

Van Geel et al. (1996) and Engels and Van Geel (2012) provide reviews of the spatial extent of changes in the hydrological cycle and conclude that this climate change is recognizable in Ireland, the United Kingdom, Germany, and further east to the Czech Republic and north to Fennoscandia, and that the combined evidence suggests a large-scale reorganization of atmospheric circulation patterns around 2800 cal. yr BP. Van Geel et al. (1996) observed that the Subboreal/Subatlantic transition occurs during a time of low solar activity, as recognized in the record of past atmospheric  $^{14}\text{C}$  levels (the  $\Delta^{14}\text{C}$ -record that can be derived from the so-called calibration curve after correction for radioactive decay; Reimer et al., 2013). Martín-Puertas et al. (2012) combined  $^{10}\text{Be}$  analysis (another proxy for solar activity) with detailed reconstructions of climate change using a high-resolution sedimentary record from Meerfelder Maar (Germany). Their results showed a change in atmospheric circulation patterns that occurred abruptly and in phase with the occurrence of a grand solar minimum, and provided convincing evidence for solar variability as the main driver of climate change at 2800 cal. yr BP. A change in atmospheric circulation patterns may also have been the driver of the change toward less negative  $\delta\text{D}$  values which we observed to have started during Phase II and which persisted during phase III. In this scenario, a shift in moisture source region closer to Uddelermeer or a more direct pathway of moisture to Uddelermeer could have resulted in a decreased amount of rain-out during moisture transport, resulting in less negative precipitation- $\delta\text{D}$  values.

**Phase IV: Present-day lake-level lowstand (58–0 cm depth; 60 cal. yr BP – present).** It is hard to identify the main driver of the lake-level lowering at the onset of Phase IV, as the exact timing of this event remains unclear. The most likely scenario is that increased human impact on the local hydrology was the main reason for the local lowering of the groundwater levels. Groundwater is currently used for irrigation during dry periods. This, together with the effects of the construction of drainage systems, has led to a significant drop in groundwater tables in the course of the 20th century. Additionally, the basal date of the outflow situated on the south end of the lake together with the rather straight shape of the current outflow suggests active management of the surface waters as well.

## Conclusion

Uddelermeer is a unique lake for The Netherlands, containing a sediment record that continuously registered environmental and climatic change from the late glacial to the present. We retrieved a 15.6-m-long sediment record from the deepest part of the sedimentary basin and developed an age–depth model for the record using a combination of radiocarbon dating,  $^{210}\text{Pb}$  dating, and Bayesian modeling. Using a novel combination of palaeoecological proxies (e.g. chironomids), quantitative estimates of change (GPR), and estimates of changes in precipitation (lipid biomarker  $\delta\text{D}$ ), we conclude the following:

- Lake levels were at least as high as present-day water levels from the late glacial to 3150 cal. yr BP, with the exception of a lake-level lowstand during the Preboreal period. A similar lake-level lowstand is also observed at other sites from The Netherlands.
- Lake levels were ~2.5 m lower than at present between 3150 and 2800 cal. yr BP, a result that was also found for a set of lakes in the French Alps (Magny, 2004). The lake-level lowering might have been the result of a change in atmospheric circulation, as a change toward less negative  $\delta\text{D}$  values of terrestrial lipid biomarker  $n\text{C}_{29}$  is interpreted to have been the result of changes in moisture source region. Alternatively, local factors such as an erosional outflow event or increasing human influence on the local hydrology toward the end of the Bronze Age could explain the lake-level lowering.
- Increasing precipitation amounts from 2800 cal. yr BP onward resulted in a rise in lake levels by about 3.5–4 m to levels that were 1–1.5 m higher than at present. The reconstructed highstand is in line with increased precipitation levels as reconstructed from nearby raised bog areas as well as with reconstructions from other European sites.
- Lake levels decreased to their present levels only during recent times, although the exact timing of the fall in lake levels is unclear. It is likely that agricultural activities and other human influences on the local hydrological system caused this decrease.

Summarizing, we reconstructed a dynamic lake-level history for Uddelermeer with a, for The Netherlands, previously unrecognized phase of lowered lake levels between 3150 and 2800 cal. yr BP. We show that the subfossil chironomid fauna of a shallow lake can be used as an indicator of past changes in lake levels of shallow lakes, especially when combined with quantitative indicators of past lake levels such as GPR imaging. The analyses of stable isotope ratios (in our case compound-specific  $\delta\text{D}$  values of a lipid biomarker derived from terrestrial plants) provide a valuable new tool in identifying potential drivers of changes in lake level as derived from palaeoecological and sedimentological indicators.

## Acknowledgements

We thank the following people for their contribution to this study: Nelleke van Asch, Erik J de Boer, Remko Engels, Andy F Lotter, Julia Sassi, and Hessel Woolderink for help during fieldwork; Annemarie Philip for preparing pollen samples; and Christopher Bronk Ramsey, Johannes van der Plicht, and Christine S Lane for help with the chronological work. We thank the two anonymous reviewers for their suggestions that helped improve this manuscript. Tieke Poelen and Kroondomein Het Loo are thanked for granting permission to access the site.

## Funding

The research of SE is financed by the Netherlands Organisation for Scientific Research (NWO, project 863.11.009).

## References

- Alley RB and Cuffey KM (2001) Oxygen- and hydrogen-isotopic ratios of water in precipitation: Beyond paleothermometry. *Reviews in Mineralogy and Geochemistry* 43: 527–553.
- Bennett KD (1996) Determination of the number of zones in a biostratigraphical sequence. *New Phytologist* 132: 155–170.
- Beug H (2004) *Leitfaden der Pollenbestimmung für Mitteleuropa und angrenzende Gebiete*. München: Verlag Dr. Friedrich Pfeil.
- Birks HJB, Heiri O, Seppä H et al. (2010) Strengths and weaknesses of quantitative climate reconstructions based on late-Quaternary biological proxies. *The Open Ecology Journal* 3: 68–110.
- Bohncke SJP (1991) *Palaeohydrological Changes in the Netherlands during the Last 13000 Years*. PhD Thesis, Vrije Universiteit Amsterdam.
- Bohncke SJP and Wijnstra T (1988) Reconstruction of Late-Glacial lake-level fluctuations in The Netherlands based on palaeobotanical analyses, geochemical results and pollen-density data. *Boreas* 17: 403–425.
- Bos JAA, Bohncke SJP and Jansen CR (2006) Lake-level fluctuations and small-scale vegetation patterns during the late glacial in The Netherlands. *Journal of Paleolimnology* 35: 211–238.
- Bos JAA, van Geel B, van der Plicht J et al. (2007) Preboreal climate oscillations in Europe: Wiggle-match dating and synthesis of Dutch high-resolution multi-proxy records. *Quaternary Science Reviews* 26: 15–16.
- Bronk Ramsey C (2009) Bayesian analysis of radiocarbon dates. *Radiocarbon* 51: 337–360.
- Brooks SJ, Langdon PG and Heiri O (2007) *The Identification and Use of Palaeo-archaic Chironomidae Larvae in Palaeoecology* (Quaternary Research Association Technical Guide No. 10). London: Quaternary Research Association.
- Dahl SO and Nesje A (1992) Palaeoclimatic implications based on equilibrium-line altitude depressions of reconstructed Younger Dryas and Holocene cirque glaciers in inner Nordfjord, western Norway. *Palaeogeography, Palaeoclimatology, Palaeoecology* 94: 87–97.
- Digerfeldt G (1986) Studies on past lake-level fluctuations. In: Berglund BE (ed.) *Handbook of Holocene Palaeoecology and Palaeohydrology*. Chichester: John Wiley & Sons, pp. 127–142.
- Dupont LM (1985) *Temperature and rainfall variation in a raised bog ecosystem*. PhD Thesis, Universiteit van Amsterdam.
- Engels S and Cwynar LC (2011) Changes in fossil chironomid remains along a depth gradient: Evidence for common faunal breakpoints within lakes. *Hydrobiologia* 665: 15–38.
- Engels S and Van Geel B (2012) The effects of changing solar activity on climate: Contributions from palaeoclimatological studies. *Journal of Space Weather and Space Climate* 2: A09.
- Engels S, Cwynar LC, Shuman BN et al. (2012) Chironomid-based lake depth reconstructions: An independent evaluation of site-specific and local inference models. *Journal of Paleolimnology* 48: 693–709.
- Faegri K and Iversen J (1989) *Textbook of Pollen Analysis*. Chichester: John Wiley & Sons.
- Garcin Y, Schefuß E, Schwab VF et al. (2014) Reconstructing C3 and C4 vegetation cover using n-alkane carbon isotope ratios in recent lake sediments from Cameroon, Western Central Africa. *Geochimica et Cosmochimica Acta* 142: 482–500.
- Grimm EC (1993) *Tilia*. Springfield, IL: Illinois State Museum.
- Grimm EC (2004) *TGView*. Springfield, IL: Illinois State Museum.
- Heidinga HA (1987) The Hunneschans at Uddel reconsidered: Some ideas about the function of a medieval ringfort in the central Netherland. In: Flambard Héricher A-M (ed.) *Château Gaillard. Études de castellologie médiévale Bd. 13*. Gent: Publications du Centre de Recherches Archéologiques et Historiques Médiévales, pp. 53–62.
- Heiri O, Cremer H, Engels S et al. (2007) Late-Glacial summer temperatures in the Northwest European lowlands: A new chironomid record from Hijkermeer, the Netherlands. *Quaternary Science Reviews* 26: 2420–2437.
- Heiri O, Lotter AF and Lemcke G (2001) Loss on ignition as a method for estimating organic and carbonate content in sediments: Reproducibility and comparability of results. *Journal of Paleolimnology* 25: 101–110.
- Hoek WZ (1997) Late-glacial and early Holocene climatic events and chronology of vegetation development in the Netherlands. *Vegetation History and Archaeobotany* 6: 197–213.
- Hoek WZ (2001) Vegetation response to the ~14.7 and ~11.5 ka cal BP climate transitions: Is vegetation lagging climate? *Global and Planetary Change* 30: 103–115.
- Hoek WZ and Bohncke SJP (2002) Climatic and environmental events over the Last Termination, as recorded in The Netherlands: A review. *The Netherlands Journal of Geosciences* 81: 123–137.
- IPCC (2013) *Climate Change 2013: The Physical Science Basis*. Cambridge: Cambridge University Press.
- Jansen B, Hausmann NS, Tonnejck FH et al. (2008) Characteristic straight-chain lipid ratios as a quick method to assess past forest – Páramo transitions in the Ecuadorian Andes. *Palaeogeography, Palaeoclimatology, Palaeoecology* 262: 129–139.
- Juggins S (2003) *C2 User Guide. Software for Ecological and Palaeoecological Data Analysis and Visualisation*. Newcastle upon Tyne: University of Newcastle.
- Kilian MR, van der Plicht J and van Geel B (1995) Dating raised bogs: New aspects of AMS <sup>14</sup>C wiggle matching, a reservoir effect and climatic change. *Quaternary Science Reviews* 14: 959–966.
- Lotter AF and Juggins S (1991) POLPROF, TRAN and ZONE: Programs for plotting, editing and zoning pollen and diatom data. *INQUA-Subcommission for the Study of the Holocene, Working Group on Data-Handling Methods, Newsletter* 6: 4–6.
- Lotter AF, Eicher U, Siegenthaler U et al. (1992) Late-glacial climatic oscillations as recorded in Swiss lake sediments. *Journal of Quaternary Science* 7: 187–204.
- Magny M (1993) Solar influences on Holocene climatic changes illustrated by correlations between past lake-level fluctuations and the atmospheric <sup>14</sup>C record. *Quaternary Research* 40: 1–9.
- Magny M (2004) Holocene climate variability as reflected by mid-European lake-level fluctuations and its probable impact on prehistoric human settlements. *Quaternary International* 113: 65–79.
- Magny M (2006) Holocene fluctuations of lake levels in West-Central Europe: Methods of reconstruction, regional pattern,

- palaeo-climatic significance and forcing factors. In: Elias SA (ed.) *Encyclopedia of Quaternary Geology*. Amsterdam: Elsevier, pp. 1389–1399.
- Magny M (2013) Climatic and environmental changes reflected by lake-level fluctuations at Gerzensee from 14,850 to 13,050 yr BP. *Palaeogeography, Palaeoclimatology, Palaeoecology* 391: 33–39.
- Magny M and Bégeot C (2004) Hydrological changes in the European midlatitudes associated with freshwater outbursts from Lake Agassiz during the Younger Dryas event and the early Holocene. *Quaternary Research* 61: 181–192.
- Mangerud J, Andersen ST, Berglund BE et al. (1974) Quaternary stratigraphy of Norden, a proposal for terminology and classification. *Boreas* 3: 109–128.
- Martín-Puertas C, Matthes K, Brauer A et al. (2012) Regional atmospheric circulation shifts induced by a grand solar minimum. *Nature Geoscience* 5: 397–401.
- Moore PD, Webb JA and Collinson ME (1991) *Pollen Analysis*. Malden, MA: Blackwell.
- Nevalainen L and Luoto TP (2012) Intralake training set of fossil Cladocera for Paleohydrological inferences: Evidence for multicentennial drought during the Medieval Climate Anomaly. *Ecohydrology* 5: 834–840.
- Newby PE, Donnelly JP, Shuman BN et al. (2009) Evidence of centennial-scale drought from southeastern Massachusetts during the Pleistocene/Holocene transition. *Quaternary Science Reviews* 28: 1675–1692.
- Oksanen J, Guillaume Blanchet F, Kindt R et al. (2015) *VEGAN: Community Ecology Package* (R package version 2.2–1). Available at: <http://CRAN.R-project.org/package=vegan>.
- Punt W and Clarke GCS (1984) *The Northwest European Pollen Flora, IV*. Amsterdam: Elsevier.
- R Development Core Team (2010) *R: A Language and Environment for Statistical Computing*. Vienna: R Foundation for Statistical Computing.
- Rach O, Brauer A, Wilkes H et al. (2014) Delayed hydrological response to Greenland cooling at the onset of the Younger Dryas in Western Europe. *Nature Geoscience* 7: 109–112.
- Reimer PJ, Bard E, Bayliss A et al. (2013) IntCal13 and Marine13 Radiocarbon Age calibration curves 0–50,000 years cal BP. *Radiocarbon* 55: 1869–1887.
- Sachse D, Billault I, Bowen GJ et al. (2012) Molecular paleohydrology: Interpreting the hydrogen-isotopic composition of lipid biomarkers from photosynthesizing organisms. *Annual Reviews in Earth and Planetary Science* 40: 221–249.
- Sachse D, Radke J and Gleixner G (2004) Hydrogen isotope ratios of recent lacustrine sedimentary n-alkanes record modern climate variability. *Geochimica et Cosmochimica Acta* 68: 4877–4889.
- Sanchez-Cabeza JA and Ruiz-Fernández AC (2012) <sup>210</sup>Pb sediment radiochronology: An integrated formulation and classification of dating models. *Geochimica et Cosmochimica Acta* 82: 183–200.
- Shuman BN, Newby P and Donnelly JP (2009) Abrupt climate change as an important agent of ecological change in the northeast US throughout the past 15,000 years. *Quaternary Science Reviews* 28: 1693–1709.
- Shuman BN, Newby P, Huang Y et al. (2004) Evidence for the close climatic control of New England vegetation history. *Ecology* 85: 1297–1310.
- Slicher van Bath BH (1987) *Agrarische Geschiedenis van West-Europa (500–1850)*. Utrecht: Het Spectrum.
- Stockmarr J (1971) Tablets with spores used in absolute pollen analysis. *Pollen et Spores* 13: 615–621.
- Van Eeden FW (1886) *Onkruid. Botanische wandelingen van F.W. van Eeden*. Haarlem: Tjeenk Willink.
- Van Geel B (1978) A palaeoecological study of Holocene peat bog sections in Germany and the Netherlands. *Review of Palaeobotany and Palynology* 25: 1–120.
- Van Geel B, Bohncke SJP and Dee H (1981) A palaeoecological study of an upper late glacial and Holocene sequence from ‘De Borchert’, The Netherlands. *Review of Palaeobotany and Palynology* 31: 367–448.
- Van Geel B, Buurman J and Waterbolk HT (1996) Archeological and palaeoecological indications of an abrupt climate change in The Netherlands, and evidence for climatological teleconnections around 2650 BP. *Journal of Quaternary Science* 11: 451–460.
- Van Geel B, Coope GR and Van der Hammen T (1989) Palaeoecology and stratigraphy of the lateglacial type section at Usselo (The Netherlands). *Review of Palaeobotany and Palynology* 60: 25–129.
- Van Geel B, Heijnis H, Charman DJ et al. (2014) Bog burst in the eastern Netherlands triggered by the 850 BC climate event. *The Holocene* 24: 1465–1477.
- Van Geel B, Van der Plicht J, Kilian MR et al. (1998) The sharp rise of  $\Delta^{14}\text{C}$  ca. 800 cal BC: Possible causes, related climatic teleconnections and the impact on human environments. *Radiocarbon* 40: 535–550.
- Wohlfarth B, Gaillard M-J, Haeberli W et al. (1994) Environment and climate in southwestern Switzerland during the Last Termination, 15–10 ka BP. *Quaternary Science Reviews* 13: 361–394.
- Zhang X, Zwiers FW, Hegerl GC et al. (2007) Detection of human influence on twentieth-century precipitation trends. *Nature* 448: 461–465.